

THEORY OF THE MESIC AUGER EFFECT

by

ELIZABETH ANN MILLER

B.Sc., University of Victoria, 1971

A THESIS SUBMITTED IN PARTIAL FULFILLMENT
OF THE REQUIREMENTS FOR THE DEGREE OF
MASTER OF SCIENCE

in the Department

of

Physics

ACCEPTED
FACULTY OF GRADUATE STUDIES

DEAN

DATE JUL 23 1979

We accept this thesis as conforming
to the required standard

Dr. C.S. Wu

Dr. C.E. Picciotto

Dr. W.J. Balfour

Dr. J.T. Weaver

© ELIZABETH ANN MILLER
UNIVERSITY OF VICTORIA

April 1979

All rights reserved. This thesis may not be reproduced in whole or in part, by mimeograph or other means, without the permission of the author.

Supervisor: Professor C. S. Wu

PAGE

Abstract..... 11

Table of Contents..... iii-iv

List of Tables..... v-vi

List of Figures..... vii

Chapter

ABSTRACT

THEORY OF THE MESIC AUGER EFFECT

The non-relativistic formulae for the Mesic Auger Effect have been extended and modified. A general formula has been developed which is applicable to transitions of any multipolarity and which also contains the penetration terms. Calculations have been performed, and both penetration terms and the higher multipole transitions have been found to be significant when the "meson" is in a state of high principal quantum number.

[Redacted]

Dr. C. S. Wu

[Redacted]

Dr. C. E. Picciotto

[Redacted]

Dr. W. J. Balfour

[Redacted]

Dr. J. T. Weaver

4.3 The Dipole Transition Rate Formula... 58

TABLE OF CONTENTS

5.	The Present Results	
5.1	The Total Transition Rate.....	60
5.2	Monopole Transition Rates.....	
		PAGE
	Abstract.....	ii
	Table of Contents.....	iii -iv
	List of Tables.....	v-vi
	List of Figures.....	vii
	Chapter	
1.	Introduction	73
1.1	The Auger Effect.....	1
1.2	Mesic Atoms.....	3
1.3	Cascade.....	7
1.4	Motivation for the Present Study.....	9
2.	Past Work on the Internal Mesic Auger Effect	89
2.1	Introduction.....	10
2.2	Monopole Transitions.....	14
2.3	Dipole Transitions.....	16
2.4	The Higher Multipole Terms and Condo's Trapping Argument.....	18
3.	Development of the General Formula	
3.1	Wave Functions.....	22
3.2	Integration over the Angular Variables	26
3.3	Integration over the Radial Variables	28
4.	The Present Work. Formulae	
4.1	The General Transition Rate Formula..	52
4.2	The monopole Transition Rate Formula.	56
4.3	The Dipole Transition Rate Formula...	58

5.	The Present Work. Numerical Results	
	5.1 The Total Transition Rate.....	60
TABLE	5.2 Monopole Transition Rates.....	64
	5.3 Dipole Transition Rates.....	67
I	5.4 Higher Multipole Rates.....	71
II	5.5 The Dipole, Quadrupole and Octopole	
III	Transition Rates as a Function of	
	$n_{\pi i}$ and $l_{\pi i}$	73
IV	5.6 Transition Rates as a Function of	
	$(n_{\pi i} - n_{\pi f})$	83
V	5.7 The Role of the Penetration Terms for	
	Dipole Transition Rates.....	86
	5.8 Conclusions and Recommendations.....	89
	References.....	91
	Appendices	
	A. Introduction to Hypergeometric Functions	
	B. Energies and Screening Factors for Some	66
VII	Circular Orbits of Pionic Helium.	
	Contribution of the Dipole [$\Delta l = -1$] Transition	
	Rate [$\omega_{\Delta l = -1}$] to the Total Transition	
	Rate [ω_T] as a Function of $n_{\pi i}$ and $l_{\pi i}$	43
VIII	Contribution of the Dipole [$\Delta l = +1$] Transition	
	Rate [$\omega_{\Delta l = +1}$] to the Total Transition	
	Rate [ω_T] as a Function of $n_{\pi i}$ and $l_{\pi i}$	69
IX	Contribution of the Quadrupole [$\Delta l = +2$]	
	Transition Rate [$\omega_{\Delta l = +2}$] to the Total Transition	
	Rate [ω_T] as a Function of $n_{\pi i}$ and $l_{\pi i}$	74

LIST OF TABLES

TABLE		PAGE
I	Particle Properties	5
II	Mesic Atom Properties	6
III	The Total Auger Transition Rate, ω_T , as a Function of $n_{\pi i}$ and $l_{\pi i}$	62
IV	ω_0/ω_T , where ω_0 is the Sum of the Two Dipole Transitions into the Highest Allowed Orbit as a Function of $n_{\pi i}$ and $l_{\pi i}$	63
V	Contribution of the Monopole Transitions [$\omega_{\Delta l=0}$] to the Total Transition Rate [ω_T] as a Function of $n_{\pi i}$ and $l_{\pi i}$	65
VI	Monopole Transitions into Circular Orbits as Compared to Dipole Transitions into the Same Orbit	66
VII	Contribution of the Dipole [$\Delta l_{\pi} = -1$] Transition Rate [$\omega_{\Delta l=-1}$] to the Total Transition Rate [ω_T] as a Function of $n_{\pi i}$ and $l_{\pi i}$.	68
VIII	Contribution of the Dipole [$\Delta l = +1$] Transition Rate [$\omega_{\Delta l=+1}$] to the Total Transition Rate [ω_T] as a Function of $n_{\pi i}$ and $l_{\pi i}$	69
IX	Contribution of the Quadrupole [$\Delta l = +2$] Transition Rate [$\omega_{\Delta l}$] to the Total Transition Rate [ω_T] as a Function of $n_{\pi i}$ and $l_{\pi i}$.	74

X	Contribution of the Octopole [$\Delta l_{\pi} = +3$]	
	Transition Rate [$\omega_{\Delta l}$] to the Total Transition	
FIGURE	Rate [ω_T] as a Function of $n_{\pi i}$ and $l_{\pi i}$	PA 75
XI	The Transition Rate for $\Delta n_{\pi} = \Delta l_{\pi} = -1$	
1.	Transitions as a Function of $n_{\pi i}$ and $l_{\pi i}$	76
XII	The Transition Rate for $\Delta n_{\pi} = \Delta l_{\pi} = -2$	11
2.	Transitions as a Function of $n_{\pi i}$ and $l_{\pi i}$	77
XIII	The Transition Rate for $\Delta n_{\pi} = \Delta l_{\pi} = -3$	11
3.	Transitions as a Function of $n_{\pi i}$ and $l_{\pi i}$	78
XIV	The Contribution to the Total Transition Rate	
	from the Transitions into the Highest	
	Allowed Orbit.	70
4.	Dependence of the Transition Rate on Multipolarity	85
	for $n_{\pi i} = 7$	79
5.	Dependence of the Transition Rate on Multipolarity	
	for $n_{\pi i} = 13$	80
6.	Expanded View of the Case Displayed in Figure 5	81
7.	Dependence of the Transition Rate on Multipolarity	
	for $n_{\pi i} = 17$	82
8.	Branching Ratios for Auger Transitions from the	
	$n_{\pi i} = 17, l_{\pi i} = 0$ State	83
9.	The Penetration Factor $P = \omega/\omega_n \approx 1$ as a function	
	of $n_{\pi i}$ and $l_{\pi i}$ for Dipole Transitions	88

LIST OF FIGURES

CHAPTER 1

INTRODUCTION

FIGURE	PAGE
1.	Distance Between Two Points Having a Common Origin
1.1	The Auger Effect
2.	Regions of Convergence of the One-Center Expansion
3.	Examples of Branching Ratios of Auger Transitions Indicating the Tendency Away from the Circular Orbits
4.	Dependence of the Transition Rate on Multipolarity for $n_{\pi i} = 7$
5.	Dependence of the Transition Rate on Multipolarity for $n_{\pi i} = 13$
6.	Expanded View of the Case Displayed in Figure 5
7.	Dependence of the Transition Rate on Multipolarity for $n_{\pi i} = 17$
8.	Branching Ratios for Auger Transitions from the $n_{\pi i} = 17, \ell_{\pi i} = 0$ State
9.	The Penetration Factor $P = \omega/\omega_n - 1$ as a function of $n_{\pi i}$ and $\ell_{\pi i}$ for Dipole Transitions

CHAPTER 1

INTRODUCTION

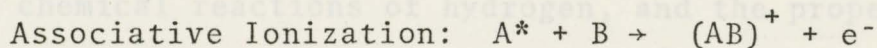
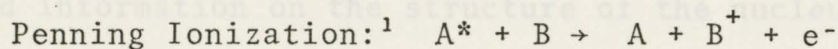
1.1 The Auger Effect

In the years 1925-26, P. Auger irradiated inert gases contained in a Wilson Cloud-chamber with a beam of x-rays and observed paired electron tracks originating from some of the ionized atoms. In each of these pairs, one track represented the photo-electron and had a variable length depending on the energy of the ionizing radiation. The other track had a constant length and represented the radiationless reorganization of the atom now named after Auger. In 1927, G. Wentzel gave the non-relativistic theory of the Auger Effect, explaining it as an autoionizing process resulting from the electrostatic interaction between two electrons in an atom which already has a vacancy in an inner shell.

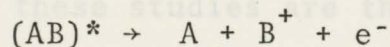
The Auger Effect and the ordinary quantized emission of radiation are the two principal processes whereby an atom in an excited state may proceed to a state of lower energy. Radiative transitions are usually limited to those transitions involving a change in orbital angular momentum of one unit, the photon having spin one; however, they are not limited by the magnitude of the energy available for

the transition. In contrast, Auger transitions occur only when the ionization potential can be overcome, yet are not restricted by angular momentum considerations and hence may occur for other than dipole transitions.

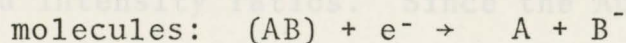
Related to the Auger Effect are processes involving more than one atom; these are collectively known as Chemionization. These are collision processes resulting in ionization, but where the collision energy is too small to overcome the ionization potential. Examples are



Preionization of diatomic molecules;



Dissociative attachment of electrons to diatomic



All these radiationless transitions, Auger and Chemionization, are characterized by the coupling of a discrete state and a continuous state of the same energy.

¹In the study of mesic atoms, this is referred to as the external Auger Effect.

1.2 Mesic Atoms

Many of the elementary particles are electrically charged. This enables them to become incorporated in an atom, a negatively charged particle replacing an electron to form a mesic atom.¹ Although the mean lifetimes of these elementary particles are very short, 10^{-6} - 10^{-10} seconds, this still exceeds the time required for many atomic transitions, 10^{-10} - 10^{-15} seconds; hence the detailed study of such atoms is possible. Such studies yield information on the structure of the nucleus, the fast chemical reactions of hydrogen, and the properties of the elementary particles themselves. The central sources of information for these studies are the binding energies of the elementary particles, the x-ray line widths and intensity ratios. Since the Auger Effect competes with the radiative process, it must necessarily be included in any attempt to theoretically justify the experimental data.

Among the most commonly studied mesic atoms are the muonic, pionic, and kaonic atoms. A review of the basic properties of the pion, muon, and kaon and the atoms they form can be found in Tables I and II.

In a mesic atom the energy level structure is analo-

¹The term "mesic" atom is commonly used to refer to all such atoms even when the particle is not a true meson.

gous to that of the electron in a normal hydrogen atom. The quantum numbers, n and ℓ , affecting the orbital motion apply. Since the muon has spin $\frac{1}{2}\hbar$, muonic atoms also have the same quantum number, j , for the total angular momentum. However, for pionic and kaonic atoms, $j = \ell$, as the pion and kaon have spin $0\hbar$.

Pionic and kaonic atoms differ strikingly from muonic and electronic atoms however, since the pions and kaons interact strongly with the nucleus. This interaction shifts the energy levels of the particles and also greatly depopulates the lower energy levels as the particles come into contact with and are absorbed by the nucleus.

TABLE I

PARTICLE PROPERTIES

PARTICLE	MEAN LIFETIME	MASS	SPIN	CHARGE	DECAY MODE	STRONG INTERACTION
MUON	2.20×10^{-6} sec	105.66 Mev $-207 m_e$	$\frac{1}{2}$	$-e$	$\mu \rightarrow e + \bar{\nu}_e + \nu_\mu$	NO
PION	2.60×10^{-8} sec	139.57 Mev $-273 m_e$	0	0	$\pi \rightarrow \mu + \nu_\mu$ $\pi \rightarrow \rho + \nu_\mu + \nu_\mu$	YES

TABLE I

PARTICLE PROPERTIES

PARTICLE	MUON	PION	KAON	ELECTRON
MEAN LIFETIME	2.20×10^{-6} sec	2.60×10^{-8} sec	1.24×10^{-8} sec	∞
MASS (in Rydbergs) ²	105.66 Mev = 207 m_e	139.57 Mev = 273 m_e	493.67 Mev = 966 m_e	.511 Mev = m_e
SPIN	$\frac{1}{2}\hbar$	0	0	$\frac{1}{2}\hbar$
CHARGE	-e	-e	-e	-e
DECAY MODE	$\mu^- \rightarrow e^- + \bar{\nu}_e + \nu_\mu$	$\pi^- \rightarrow \mu^- + \bar{\nu}_\mu$	$\kappa^- \rightarrow \mu\nu$ $\pi\pi_0$ $\pi\pi^+\pi^-$...	stable
STRONG INTERACTION	NO	YES	YES	NO

¹without corrections for reduced mass, nuclear size, vacuum polarization, and strong interaction effect

²1 Rydberg = $(e^2/2a_0) = 13.6$ ev

TABLE II

MESIC ATOM PROPERTIES¹

PARTICLE	MUON	PION	KAON	ELECTRON
E_n (in Rydbergs) ²	$-\left(\frac{m_\mu}{m_e}\right) \frac{Z^2}{n^2} = -207 \frac{Z^2}{n^2}$	$-\left(\frac{m_\pi}{m_e}\right) \frac{Z^2}{n^2} = -273 \frac{Z^2}{n^2}$	$-\left(\frac{m_K}{m_e}\right) \frac{Z^2}{n^2} = -966 \frac{Z^2}{n^2}$	$-\frac{Z^2}{n^2}$
$\langle r_{n,l} \rangle$	$\langle r_{n,l} \rangle_e / (207)$	$\langle r_{n,l} \rangle_e / (273)$	$\langle r_{n,l} \rangle_e / (966)$	$\langle r_{n,l} \rangle_e =$ $= \frac{a_0}{2Z} \{3n^2 - l(l+1)\}$
VALUES OF n SUCH THAT $\langle r_{n,l} \rangle_\pi \approx \langle r_{1,0} \rangle_e$	14 - 17	17 - 20	31 - 38	1

¹without corrections for reduced mass, nuclear size, vacuum polarization, and strong interaction effect

²1 Rydberg = $(e^2/2a_0) = 13.6$ eV

1.3 Cascade

Consider a muon of kinetic energy ~ 100 Mev. which is produced in an accelerator and which then enters a moderator. By electromagnetic interactions with the electrons of the absorber material the muon is slowed down in 10^{-11} - 10^{-9} seconds (the moderation time) to an energy of approximately 2 Kev. Its velocity then approximates the velocity of the electrons in the normal atoms.

The muon is then captured on a particular atom through electromagnetic interaction with the electrons of that atom. The capture process takes approximately 10^{-15} - 10^{-14} seconds (the capture time) and slows the muon down to zero energy.

The muon finally cascades down through hydrogen-like bound states and eventually reaches the 1s ground state, where it stays until it decays or is absorbed by the nucleus (cascade time $\sim 10^{-12}$ sec.)

The processes by which the muon (or other particle) cascades down to the ground state (or is absorbed by the nucleus) are of intense interest in the study of mesic atoms. It is by a thorough and accurate understanding of these various processes that atomic effects can be separated from nuclear effects in the analysis of line widths and x-ray intensity ratios of the mesic atom.

As already mentioned the two principal processes by which the meson de-excites are the Auger Effect and x-ray

emission. In general, when the Auger Effect is possible (i.e. there are electrons present which can be ejected), then the Auger Effect is the dominant process for the higher n states, while the emission of x-rays is dominant for the lower n states. However in fluids, other effects — such as the external Auger Effect, in which electrons of neighboring atoms are ejected, and the Stark Effect and sliding transitions, in which angular momentum states are mixed via collision processes — are also present.

proximation to the Coulomb wave functions, while the dipole transition rate formula had been restricted to the non-penetration approximation.

The transition rate formulae for the higher multipole transitions had not been calculated, but had been assumed to be considerably smaller.

In addition, previous work was restricted to the ejection of an electron from a state of low principal quantum number ($n_0 = 1, 2$). In the present work a general formula has been developed to allow not only for any multipolarity of basic transitions, but also for the ejection of an electron from an arbitrary initial state.

Unfortunately this last step has made the derivation of the formula almost totally unreadable, plunging it into the darkest depths of series upon series of hypergeometric functions.

All numerical work has been carried out for pionic Helium with the ejection of an electron from the $1s$ state.

1.4 Motivation for the Present Study

The main focus of the present work has been to refine and extend the currently used formulae for the Mesic Auger Effect.

Until now, the only formulae which had been developed were for monopole and dipole transitions, and these were based on certain approximations. The monopole transition rate formula had been developed using the plane wave approximation to the Coulomb wave functions, while the dipole transition rate formula had been restricted to the no-penetration approximation.

The transition rate formulae for the higher multipole transitions had not been calculated, but had been assumed to be considerably smaller.

In addition, previous work was restricted to the ejection of an electron from a state of low principal quantum number ($n_e = 1, 2$). In the present work a general formula has been developed to allow not only for any multipolarity of mesic transitions, but also for the ejection of an electron from an arbitrary initial state.

Unfortunately this last step has made the derivation of the formula almost totally unreadable, plunging it into the darkest depths of series upon series of hypergeometric functions.

All numerical work has been carried out for pionic Helium with the ejection of an electron from the $1s$ state.

CHAPTER 2

PAST WORK ON THE INTERNAL MESIC AUGER FORMULAE

2.1 Introduction

The probability of a discrete autoionizing state making the transition to the continuous state of the same energy is given by Fermi's Golden Rule No. 2

$$\omega = \frac{2\pi}{\hbar} \rho(k) |\langle f | H' | i \rangle|^2 \quad (2.1)$$

where $\rho(k)$ is the density of final states, and H' is the perturbing potential. $\rho(k)$ is $m_e \hbar k / (2\pi \hbar)^3$ and, in effect, normalizes the continuum wave function to represent one electron ejected per unit energy interval.

For the Auger Effect, H' is the electrostatic potential between the two interacting electrons (i.e. the one which descends to a lower orbit and the one which is ejected). For the Mesic Auger Effect, it is the potential between the meson and the Auger electron. In both cases

$$H' = e^2 / |r_{12}| \quad (2.2)$$

where $|r_{12}|$ is the distance between the two particles.

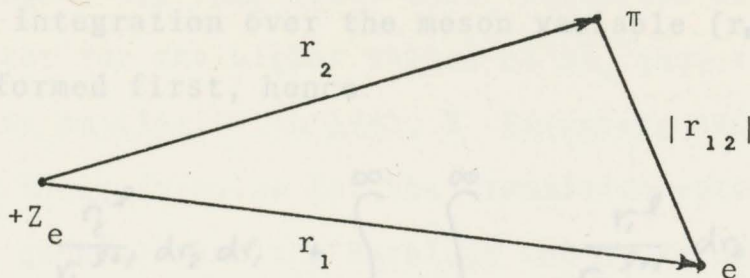


Figure 1

Distance Between Two Points Having a Common Origin

The expansion for $|r_{12}|^{-1}$ in spherical harmonics is

$$|r_{12}|^{-1} = \sum_{\ell=0}^{\infty} \sum_{m=-\ell}^{\ell} \frac{(4\pi)}{(2\ell+1)} \frac{r_{<}^{\ell}}{r_{>}^{\ell+1}} Y_{\ell}^{m*}(\Omega_1) Y_{\ell}^m(\Omega_2) \quad (2.5)$$

where

$$\frac{r_{<}^{\ell}}{r_{>}^{\ell+1}} = \begin{cases} \frac{r_1^{\ell}}{r_2^{\ell+1}} & \text{if } r_1 < r_2 \\ \frac{r_2^{\ell}}{r_1^{\ell+1}} & \text{if } r_2 < r_1 \end{cases} \quad (2.3)$$

(Messiah 1958, 497)

When performing the integrals over the radial variables, the $r_1 r_2$ plane must be divided into the two separate regions of convergence.

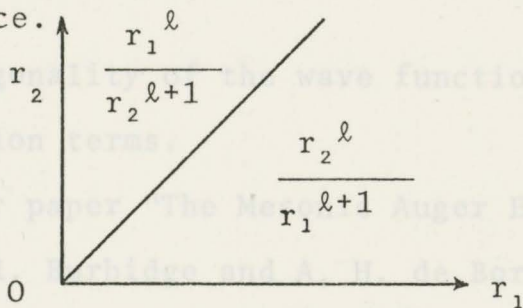


Figure 2

Regions of Convergence of the One-Center Expansion.

The integration over the meson variable (r_2) is usually performed first, hence

$$\int_{r_1=0}^{\infty} \int_{r_2=0}^{r_1} \frac{r_2^{\ell}}{r_1^{\ell+1}} dr_2 dr_1 + \int_{r_1=0}^{\infty} \int_{r_2=r_1}^{\infty} \frac{r_1^{\ell}}{r_2^{\ell+1}} dr_2 dr_1 \quad (2.4)$$

which is rearranged as

$$\int_{r_1=0}^{\infty} \int_{r_2=0}^{\infty} \frac{r_2^{\ell}}{r_1^{\ell+1}} dr_2 dr_1 + \left\{ \int_{r_1=0}^{\infty} \int_{r_2=r_1}^{\infty} \frac{r_1^{\ell}}{r_2^{\ell+1}} dr_2 dr_1 - \int_{r_1=0}^{\infty} \int_{r_2=0}^{r_1} \frac{r_2^{\ell}}{r_1^{\ell+1}} dr_2 dr_1 \right\} \quad (2.5)$$

The second and third sets of integrals are usually referred to as the penetration terms, since their contribution to the total integral depends roughly on the interpenetration of the electron and meson clouds.

For monopole transitions the first term drops out because

$$\langle \Psi_{\pi_f}(\vec{r}_2) | r_2^0 | \Psi_{\pi_i}(\vec{r}_1) \rangle \quad (2.6)$$

by the orthogonality of the wave functions, leaving only the penetration terms.

In their paper "The Mesonic Auger Effect" appearing in 1953, G. R. Burbidge and A. H. de Borde offered formulae for both monopole ($\Delta l_{\pi} = 0$) and dipole ($\Delta l_{\pi} = \pm 1$) transitions. The higher multipole transition rate formulae are

2.2 Monopole Transitions

For the monopole transitions, Burbidge and de Borde developed a formula

$$\omega = C_3^2 \frac{1}{\hbar} \left(\frac{e^2}{a_0} \right) \left(\frac{Z_e}{M Z_\pi} \right)^4 \frac{\pi e^{\pi \gamma}}{\sinh(\pi \gamma)} \frac{2^{2n+6} n^{2n+4} (n-1)^{2n+5}}{9 (2n-1)^{4n+2}} \quad (2.7)$$

which applies only to transitions where

$$(n, l = n-2) \rightarrow (n-1, l = n-2),$$

where C_3 is a constant between 0 and 1, and where γ is related to the energy of the final electron by $\gamma = +\sqrt{E}$, if E is expressed in Rydbergs.

Unfortunately, the monopole transitions are not significant for these nearly circular orbits, but are significant for transitions from orbits with high principal quantum number, n , but low angular momentum quantum number, l . Also because C_3 has such a wide range of values, this formula only sets an upper limit on the transition rate.

In 1961, Eisenberg and Kessler derived the formula

$$\omega = \frac{1}{\hbar} \left(\frac{e^2}{a_0} \right) \left(\frac{Z_e}{M Z_\pi} \right)^4 \frac{1}{8} \frac{2^{4l+7}}{3^2} \frac{(n_1+l)! (n_1-l-1)! (n_2+l)! (n_2-l-1)!}{(n_1+n_2)^{4l+10}} \cdot n_1^{2l+6} n_2^{2l+6} Q^2$$

2.3 Dipole Transitions

where

$$Q = \sum_{\lambda=0}^{n_1-l-1} \sum_{\chi=0}^{n_2-l-1} (-1)^{\lambda+\chi+1} 2^{\lambda+\chi} \frac{(\lambda+\chi+2l+2)!}{n_1^\lambda n_2^\chi \left(\frac{1}{n_1} + \frac{1}{n_2}\right)^{\lambda+\chi}} \quad (2.8)$$

$$\cdot \frac{(\lambda+\chi)(\lambda+\chi+4l+7)}{\lambda! (n_1-l-1-\lambda)! (2l+1+\lambda)! \chi! (n_2-l-1-\chi)! (2l+1+\chi)!}$$

which applied to all monopole transitions. However, they have used the plane wave approximation to the Coulomb wave function, which is a high energy approximation, and monopole transitions are dominant only for low energy (high n) transitions.

It should be noted that if the term

$$\sum_{\lambda=0}^{n_1-l-1} \sum_{\chi=0}^{n_2-l-1} (-1)^{\lambda+\chi+1} 2^{\lambda+\chi} \frac{(\lambda+\chi+2l+2)!}{n_1^\lambda n_2^\chi \left(\frac{1}{n_1} + \frac{1}{n_2}\right)^{\lambda+\chi}} \quad (2.9)$$

$$\cdot \frac{(2l+3)(2l+4)}{\lambda! (n_1-l-1-\lambda)! (2l+1+\lambda)! \chi! (n_2-l-1-\chi)! (2l+1+\chi)!} \equiv 0$$

is added to Q , then the Eisenberg and Kessler formula may be written more succinctly as

$$\omega = \frac{1}{\hbar} \left(\frac{c^2}{a_0}\right) \left(\frac{Zc}{M Z \alpha}\right)^4 \frac{1}{8} \frac{Z^3}{3^2} \left| \langle n_i, l | r^2 | n_f, l \rangle \right|^2 \quad (2.10)$$

where by $\left| \langle n_f, l_f | r^2 | n_i, l_i \rangle \right|^2$ is meant the evaluation of the integral with $a_0 = M = Z = 1$, (see Section 4.1).

2.3 Dipole Transitions

For the dipole transitions Burbidge and de Borde consider only transitions between circular orbits, that is

$$(n, l = n-1) \rightarrow (n-1, l = n-2)$$

and find

$$\omega = C^2 \frac{1}{\hbar} \left(\frac{e^2}{a_0} \right) \left(\frac{Z_e}{M Z \pi} \right)^2 \frac{\pi \gamma^2 e^{\gamma(\frac{1}{2} \tan^{-1} \gamma - \pi)}}{3(1+\gamma^2) \sinh(\pi \gamma)} \cdot \frac{2^{4n+6} n^{2n+2} (n-1)^{2n+4}}{(2n-1)^{4n+2}} \quad (2.11)$$

where

$$C = 1 - \left(\frac{Z_e}{Z \pi M} \right)^2 \frac{(1+\gamma^2)(2n+1)(2n+2)n^2(n-1)^2}{\gamma^2 e^{\gamma(\frac{1}{2} \tan^{-1} \gamma - \pi)} 3(2n-1)^2} \left(\frac{C_1}{2} - \frac{C_2}{3} \right)$$

and C_1 and C_2 are constants between 0 and 1. This formula includes the penetration terms but again there is a large uncertainty in the constants C_1 and C_2 .

There may be a simple reason that these constants C_1 and C_2 and the constant C_3 in the monopole formula were not given more precisely. For the transitions which Burbidge and de Borde examined, the monopole rates (containing the factor C_3) and the penetration contributions to the dipole rates (containing the factors C_1 and C_2) were insignificant. It was not then necessary to provide a more complicated but more precise expression for these constants.

The Eisenberg and Kessler formula for the dipole transition rates applies to all possible transitions, but does not include the penetration terms. This, again, is unfortunate as the penetration terms are significant for transitions from high n states.

$$\omega = \frac{1}{\hbar} \left(\frac{e^2}{a_0} \right) \left(\frac{Z_c}{M Z_\pi} \right)^2 \frac{\text{Max}(l_i, l_f) \pi \gamma^2 e^{\gamma(4 \tan^{-1} \gamma - \pi)}}{3(2l_f + 1)(1 + \gamma^2) \sinh(\pi \gamma)} \cdot |\langle n_f, l_f | r | n_i, l_i \rangle|^2 \quad (2.12)$$

ly, these few would decay in orbit rather than cascade down to the lower orbits, thus extending the average lifetime of a pion in helium.

For this to occur it is necessary that transitions out of these states occur only by radiative emission, while the Auger Effect, both internal and external, and the Stark Effect are inoperative. While it might be argued that, in gaseous substances, the external Auger and Stark Effects might be negligible, at that time (1964), no accurate formula for the higher multipole internal Auger rates had been developed, but only estimates had been offered.

For a pion to escape from an $n_i = 17, l_i = 16$ orbit, via an Auger transition, the pion must make a $\Delta l_i = -3, \Delta n_i = -3$ transition, which Condo assumes has a rate not greater than 10^{-4} transitions per second, the radiative rate.

2.4 The Higher Multipole Terms and Condo's Trapping

Argument

In 1964, G. T. Condo, noticing the disagreement between the theoretical and observed lifetimes of pions in helium, proposed a trapping mechanism, whereby pions were "trapped" in states having both high n and high ℓ values. He reasoned that if even a small percentage of the pions should enter these states and not be able to escape quickly, these few would decay in orbit rather than cascade down to the lower orbits, thus extending the average lifetime of a pion in helium.

For this to occur it is necessary that transitions out of these states occur only by radiative emission, while the Auger Effect, both internal and external, and the Stark Effect are inoperative. While it might be argued that, in gaseous substances, the external Auger and Stark Effects might be negligible, at that time (1964), no accurate formula for the higher multipole internal Auger rates had been developed, but only estimates had been offered.

For a pion to escape from an $n_{\pi} = 17$, $\ell_{\pi} = 16$ orbit, via an Auger transition, the pion must make a $\Delta\ell_{\pi} = -3$, $\Delta n_{\pi} = -3$ transition, which Condo assumes has a rate not greater than 10^8 transitions per second, the radiative rate. It might therefore be expected that the largeness

It is not obvious that the transition rate for these trapping orbits is so small. Consider the following very crude argument. If the no-penetration approximation is taken, i.e.

$$\frac{r_2^l}{r_2^{l+1}} \sim \frac{r_1^l}{r_1^{l+1}} \quad (2.13)$$

and if the calculations are restricted to circular orbits, then

$$\omega \sim \frac{1}{(2\pi)^2} \frac{1}{\hbar} \left(\frac{e^2}{a_0}\right) K \left| \langle \Psi_{e_s} | r^{-l-1} | \Psi_{e_i} \rangle \right|^2 \cdot \frac{(2l_\pi - 2l + 1)! (2l)!}{(2l+1)(2l_\pi+1)!} \left[\frac{(l_\pi)!}{l! (l_\pi - l)!} \right]^2 \left(\frac{a_0}{2\pi M}\right)^{2l} |\langle r^l \rangle|^2 \quad (2.14)$$

where by $|\langle r^l \rangle|$ is meant the evaluation of the integral over the pion wave functions with $a_0 = Z = M = 1$, and where l_π is $l_{\pi i}$. Then

$$\omega \sim \frac{1}{(2\pi)^2} \frac{1}{\hbar} \left(\frac{e^2}{a_0}\right) K \left| \langle \Psi_{e_s} | r^{-l-1} | \Psi_{e_i} \rangle \right|^2 \left(\frac{a_0}{2\pi M}\right)^{2l} \cdot \frac{(2l)! 2^{-2l-4}}{(2l+1) l!^2} \cdot \left\{ \frac{(l_\pi+1)^{2l_\pi+4} (l_\pi-l+1)^{2l_\pi+2l+2} l_\pi!^2}{(l_\pi - \frac{l}{2} + 1)^{2l_\pi+6} (l_\pi-l)!^2} \right\} \quad (2.15)$$

Now the total dependence on l_π is contained in the brackets and from this it can be seen that it is given approximately by l_π^{4l} . It might therefore be expected that the largeness

of $\ell_{\pi}^{4\ell}$ would cancel the smallness of the factor $M^{-2\ell}$. and
 Indeed when $r_{\pi} \approx r_e$,

In 1977, V. R. Akylas and P. Vogel also did calculations of $(2\ell_{\pi} + 3)(2\ell_{\pi} + 2) \approx 6M$ higher multipole rates for muonic atoms, however they did not mention whether or not they had for roughly transition rates from the higher circular orbits to be unusually low, but only stated that, in general, the $\ell_{\pi}^2 \approx M$ the higher multipole terms is minor, which is true.

so that

$$M^{-2\ell} \ell_{\pi}^{4\ell} \approx 1 \quad (2.17)$$

Therefore, it might be argued that when $\ell_{\pi i} = 17$, the higher multipole rates are (very roughly) comparable to the dipole rate, which is about 10^{14} transitions per second.

In 1970, J. E. Russell did a calculation of several of the higher multipole transition rates using numerical integration over the electron variable. His results show a monotonic decrease in the transition rates with an increase in $n_{\pi i}$. This is contrary to the argument just presented which indicates an increase in transition rates as $n_{\pi i}$ increases, and also contrary to previous work on dipole transitions which also shows an increase in the Auger rates as $n_{\pi i}$ increases. Since Russell published rates for only a few pionic transitions (only higher multipole rates) it

is not possible to compare his work with previous work and hence judge the reliability of his calculations.

In 1977, V. R. Akylas and P. Vogel also did calculations of the penetration terms and higher multipole rates for muonic atoms, however they did not mention whether or not they had found the transition rates from the higher circular orbits to be unusually low, but only stated that, in general, the role of the higher multipole terms is minor, which is true.

$$w_{l+2} d\Omega_k = \frac{2\pi}{\hbar} (2l_k + 1)^{-1} (2l_{l+2} + 1)^{-1} \sum_{m_1, m_2} |\langle \psi_{l+2}^{m_1}(\mathbf{r}) \psi_{l+2}^{m_2}(\mathbf{r}) | \frac{e^2}{|\mathbf{r}|} | \psi_l^{m_1}(\mathbf{r}) \psi_l^{m_2}(\mathbf{r}) \rangle|^2 \rho(k) d\Omega_k \quad (3.1)$$

where $\rho(k) = \pi_e \hbar k / (2\pi\hbar)^2$, hence

$$w_{l+2} d\Omega_k = \frac{1}{(2\pi)^2} \frac{1}{\hbar} \left(\frac{e^2}{a_0} \right) \kappa (2l_k + 1)^{-1} (2l_{l+2} + 1)^{-1} \sum_{m_1, m_2} |\langle \psi_{l+2}^{m_1} \psi_{l+2}^{m_2} | \frac{1}{|\mathbf{r}|} | \psi_l^{m_1} \psi_l^{m_2} \rangle|^2 d\Omega_k \quad (3.2)$$

The initial and final pion states and the initial electron state are bound orbitals and are written

CHAPTER 3

DEVELOPMENT OF THE GENERAL FORMULA

3.1 Wave Functions

The transition rate for the emission of an Auger electron into a given direction Ω_k is given by

$$\omega_{i \rightarrow f} d\Omega_k = \frac{2\pi}{\hbar} (2l_{\pi_i} + 1)^{-1} (2l_{e_i} + 1)^{-1} \cdot \sum_{\substack{m_{\pi_i} m_{e_i} \\ m_{\pi_f} m_{e_f}}} |\langle \Psi_{\pi_f}(\vec{r}_2) \Psi_{e_f}(\vec{r}_1) | \frac{e^2}{|\vec{r}_{12}|} | \Psi_{\pi_i}(\vec{r}_2) \Psi_{e_i}(\vec{r}_1) \rangle|^2 \cdot \rho(k) d\Omega_k \quad (3.1)$$

where $\rho(k) = m_e \hbar k / (2\pi \hbar)^3$, hence

$$\omega_{i \rightarrow f} d\Omega_k = \frac{1}{(2\pi)^2} \frac{1}{\hbar} \left(\frac{e^2}{a_0} \right) K (2l_{\pi_i} + 1)^{-1} (2l_{e_i} + 1)^{-1} \cdot \sum_{m_{\pi_i} m_{e_i}} |\langle \Psi_{\pi_f} \Psi_{e_f} | \frac{1}{|\vec{r}_{12}|} | \Psi_{\pi_i} \Psi_{e_i} \rangle|^2 d\Omega_k \quad (3.2)$$

The initial and final pion states and the initial electron state are bound orbitals and are written

$$\Psi_{\pi}(\vec{r}_2) = \left(\frac{M Z_{\pi}}{a_0}\right)^{3/2} \frac{2}{n_{\pi}^2} \sum_{p=0}^{n_{\pi}-l_{\pi}-1} (-1)^p \frac{[(n_{\pi}+l_{\pi})! (n_{\pi}-l_{\pi}-1)!]^{1/2}}{(n_{\pi}-l_{\pi}-1-p)! p!}$$

$$\frac{1}{(2l_{\pi}+1+p)!} \left(\frac{2 Z_{\pi} M r_2}{n_{\pi} a_0}\right)^{l_{\pi}+p}$$

$$e^{-\left(\frac{Z_{\pi} M r_2}{n_{\pi} a_0}\right)} Y_{l_{\pi}}^{m_{\pi}}(\Omega_2) \quad (3.3)$$

$$\Psi_e(\vec{r}_1) = \left(\frac{Z_e}{a_0}\right)^{3/2} \frac{2}{n_e^2} \sum_{s=0}^{n_e-l_e-1} (-1)^s \frac{[(n_e+l_e)! (n_e-l_e-1)!]^{1/2}}{(n_e-l_e-1-s)! s!}$$

$$\frac{1}{(2l_e+1+s)!} \left(\frac{2 Z_e r_1}{n_e a_0}\right)^{l_e+s}$$

$$e^{-\left(\frac{Z_e r_1}{n_e a_0}\right)} Y_{l_e}^{m_e}(\Omega_1) \quad (3.4)$$

where $M = m_{\pi}/m_e$ and $a_0 = \hbar^2/m_e e^2$

The final electron state is a continuum state and is represented by an infinite series of Coulomb wave functions.

$$\Psi_{e_f}(\vec{r}_1) = \Psi_e = e^{-\frac{1}{2}\pi\eta} \Gamma(1+i\eta) e^{i\vec{k}\cdot\vec{r}_1} {}_1F_1(-i\eta; 1; ikr - i\vec{k}\cdot\vec{r}_1) \quad (3.7)$$

$$= (kr)^{-1} \sum_{l_s=0}^{\infty} \sum_{m_s=-l_s}^{+l_s} 4\pi i^{l_s} e^{i\sigma_{l_s}}$$

$$\cdot F_{l_s}(\eta, kr) Y_{l_s}^{m_s}(\Omega_1) Y_{l_s}^{m_s*}(\Omega_2)$$

$$F_{l_s}(\eta, kr) = C_{l_s}(\eta) e^{-ikr} (kr)^{l_s+1} \cdot {}_1F_1(l_s+1-i\eta; 2l_s+2; +2ikr) \quad (3.5)$$

$$C_{l_s}(\eta) = \frac{2^{l_s} e^{-\frac{1}{2}\pi\eta} |\Gamma(l_s+1+i\eta)|}{\Gamma(2l_s+2)}$$

$$\sigma_{l_s} = \arg \Gamma(l_s+1+i\eta)$$

F_ℓ is called the Coulomb wave function. It is a real valued function and can be derived from the bound state wave function by the mapping $n \rightarrow i\eta$ and an appropriate change in normalization. \vec{k} is the wave vector of the ejected electron, and η is called Sommerfeld's parameter, being the quantity which determines the eccentricity of corresponding hyperbolic orbits in the Bohr-Sommerfeld theory. These two parameters are simply related.

$$a_0 \eta \kappa = Z Z' \quad (3.6)$$

The effective nuclear charge felt by the ejected electron is $Z = +1$, while the charge of the electron itself is $Z' = -1$, hence

$$a_0 \eta \kappa = -1 \quad (3.7)$$

Notice that for an attractive potential η is negative, while for a repulsive potential (encountered in scattering problems) η is positive. In the Burbidge and de Borde and the Eisenberg and Kessler Auger transition rate formulae $\gamma = |\eta|$ is used, while the present work uses η in the derivation of the general formula, but then uses γ in the final presentation of the formula.

For bound states, the discrete eigenvalues of energy are given by

3.2 Integration Over the Angular Variables

$$E_{\text{BOUND}} = - \frac{1}{2a_0} \left(\frac{ZZ'e}{n} \right)^2 \quad (3.8)$$

where n is an integer. For continuum states, the eigenvalues are obtained by the mapping

$$n \rightarrow i\eta \quad (3.9)$$

where η is a continuous parameter, hence

$$E_{\text{CONTINUUM}} = + \frac{1}{2a_0} \left(\frac{ZZ'e}{\eta} \right)^2 \quad (3.10)$$

If the energies are expressed in Rydbergs (one Rydberg = $(e^2/2a_0) = 13.6\text{ev}$), then

$$\bar{E}_B = - \left(\frac{ZZ'}{n} \right)^2 \quad \bar{E}_C = + \left(\frac{ZZ'}{\eta} \right)^2 \quad (3.11)$$

For the continuum state $ZZ' = -1$, hence

$$E_C = \frac{1}{\eta^2} \quad (3.12)$$

Furthermore, if $Z_{\pi f} = 2$, then

$$E_{e_s} = \frac{4M}{n\pi_s^2} - \left(\frac{Ze_i^2}{n_s^2} + \frac{Z\pi_i^2 M}{n\pi_s^2} \right) \quad (3.13)$$

$$1/\eta^2 = \frac{4M}{n\pi_s^2} - E(e_i, \pi_i)$$

3.2 Integration Over the Angular Variables

Integration over Ω_2 is performed by means of the Wigner-Eckart theorem

$$\int_{\Omega_2} Y_{l\pi_S}^{m\pi_S*}(\Omega_2) Y_l^m(\Omega_2) Y_{l\pi_i}^{m\pi_i}(\Omega_2) d\Omega_2 \quad (3.14)$$

$$= (-1)^{m\pi_S} \left[\frac{(2l+1)(2l_{\pi_S}+1)(2l_{\pi_i}+1)}{4\pi} \right]^{1/2} \begin{pmatrix} l & l_{\pi_i} & l_{\pi_S} \\ 0 & 0 & 0 \end{pmatrix} \begin{pmatrix} l & l_{\pi_i} & l_{\pi_S} \\ m & m_{\pi_i} & -m_{\pi_S} \end{pmatrix}$$

provided

$$|l_{\pi_i} - l_{\pi_S}| \leq l \leq |l_{\pi_i} + l_{\pi_S}|$$

$$l_{\pi_i} + l_{\pi_S} + l = \text{even integer}$$

$$m = m_{\pi_S} - m_{\pi_i}$$

Similarly

$$\int_{\Omega_1} Y_{le_S}^{me_S*}(\Omega_1) Y_l^{m*}(\Omega_1) Y_{le_i}^{me_i}(\Omega_1) d\Omega_1 \quad (3.15)$$

$$= (-1)^{m+me_S} \left[\frac{(2l+1)(2le_S+1)(2le_i+1)}{4\pi} \right]^{1/2} \begin{pmatrix} l & le_S & le_i \\ 0 & 0 & 0 \end{pmatrix} \begin{pmatrix} l & le_i & le_S \\ -m & me_i & -me_S \end{pmatrix}$$

provided

$$|le_i - l| \leq le_S \leq |le_i + l|$$

$$le_i + le_S + l = \text{even integer}$$

$$m = me_i - me_S$$

Note that the sum over l is now restricted to those values consistent with the triangle rule and the parity selection rule; and that the total $M = m_{e_i} + m_{\pi_i} = m_{e_f} + m_{\pi_f}$ if conserved.

Therefore

$$\left\langle \Psi_{\pi_S}(\vec{r}_2) \Psi_{e_S}(\vec{r}_1) \left| \frac{1}{|\vec{r}_{12}|} \right| \Psi_{\pi_2}(\vec{r}_2) \Psi_{e_2}(\vec{r}_1) \right\rangle$$

$$= \sum_{l_S, m_{e_S}} \sum_{l_2, m} (-1)^{m + m_{e_S} + m_{\pi_S}} \left[(2l_{e_2} + 1)(2l_{e_S} + 1)(2l_{\pi_2} + 1)(2l_{\pi_S} + 1) \right]^{\frac{1}{2}} \quad (3.16)$$

$$\cdot \begin{pmatrix} l & l_{e_2} & l_{e_S} \\ 0 & 0 & 0 \end{pmatrix} \begin{pmatrix} l & l_{e_2} & l_{e_S} \\ -m & m_{e_2} & m_{e_S} \end{pmatrix} \begin{pmatrix} l & l_{\pi_2} & l_{\pi_S} \\ 0 & 0 & 0 \end{pmatrix} \begin{pmatrix} l & l_{\pi_2} & l_{\pi_S} \\ m & m_{\pi_2} & -m_{\pi_S} \end{pmatrix} Y_{l_{e_S}}^{m_{e_S}}(\Omega_K) \quad (3.17)$$

$$\cdot \int_{r_1, r_2} R_{e_2}(r_1) R_{l_{e_S}}(r_1) R_{\pi_2}(r_2) R_{l_{\pi_S}}(r_2) \frac{r_1^l}{r_2^{l+1}} r_1^2 r_2^2 dr_1 dr_2$$

which eventually leads to

$$\omega_{2 \rightarrow S} = \frac{1}{(2\pi)^2} \frac{1}{\hbar} \left(\frac{e^2}{a_0} \right) K (2l_{e_S} + 1)^{-1} (2l_{\pi_2} + 1)^{-1} \quad (3.17)$$

$$\sum_{\substack{m_{e_2} m_{e_S} \\ m_{\pi_2} m_{\pi_S} \\ m}} \int_{\Omega_K} |\langle \Psi_S | \frac{1}{|\vec{r}_{12}|} | \Psi_2 \rangle|^2 d\Omega_K \quad (3.20)$$

$$= \frac{1}{(2\pi)^2} \frac{1}{\hbar} \left(\frac{e^2}{a_0} \right) K \sum_{l_S, l} \frac{(2l_{\pi_S} + 1)}{(2l + 1)} \begin{pmatrix} l & l_{\pi_2} & l_{\pi_S} \\ 0 & 0 & 0 \end{pmatrix}^2 \quad (3.18)$$

$$\cdot \frac{(2l_{e_S} + 1)}{(2l + 1)} \begin{pmatrix} l & l_{e_2} & l_{e_S} \\ 0 & 0 & 0 \end{pmatrix}^2 |R_{l_{e_S}, l}|^2 \quad (3.21)$$

3.3 Integration Over the Radial Variables

3.3.1 Preliminaries

$$\begin{aligned}
 R_{l_{e_3}, l} = & \left\{ 4\pi (-i)^{l_{e_3}} e^{-i\sigma l_{e_3}} C_{l_{e_3}}(r_2) K_{l_{e_3}} \right. \\
 & \cdot \left(\frac{z_c}{a_0} \right)^{3/2} \frac{2}{n_{e_3}} \sum_{s=0}^{n_{e_3}-l_{e_3}-1} (-1)^s \dots \left(\frac{2z_c}{n_{e_3} a_0} \right)^{l_{e_3} + s} \\
 & \cdot \left(\frac{Mz_{\pi}}{a_0} \right)^{3/2} \dots \left(\frac{2Mz_{\pi}}{n_{\pi_2} a_0} \right)^{l_{\pi_2} + p} \\
 & \cdot \left(\frac{Mz_{\pi}}{a_0} \right)^{3/2} \dots \left. \left(\frac{2Mz_{\pi}}{n_{\pi_3} a_0} \right)^{l_{\pi_3} + q} \right\} \quad (3.19) \\
 & \cdot \int_{r_1, r_2} c^{-ikr_1} r_1^{l_{e_3}} {}_1F_1(l_{e_3} + 1 - i\eta; 2l_{e_3} + 2; 2ikr_1) e^{-\left(\frac{z_c}{n_{e_3} a_0}\right) r_1} \\
 & \cdot r_1^{l_{e_3} + s} r_2^{l_{\pi_2} + p + l_{\pi_3} + q} e^{-\left(\frac{z_{\pi}}{n_{\pi_2}} + \frac{z_{\pi}}{n_{\pi_3}}\right) \frac{M}{a_0} r_2} \\
 & \cdot \left(\frac{r_2^l}{r_2^{l+1}} \right) r_1^2 r_2^2 dr_1 dr_2 \\
 = & \left\{ \dots \right\} \left\{ I_0(s, p, q) - I_1(s, p, q) + I_2(s, p, q) \right\}
 \end{aligned}$$

where I_1 and I_2 now represent the penetration terms.

By defining

$$A_e = \left(\frac{z_c}{n_{e_3} a_0} \right) + ik \quad L_e = l_{e_3} + l_{e_3} + s + 2 \quad (3.20)$$

$$A_{\pi} = \left(\frac{z_{\pi}}{n_{\pi_2}} + \frac{z_{\pi}}{n_{\pi_3}} \right) \frac{M}{a_0} \quad L_{\pi} = l_{\pi_2} + l_{\pi_3} + p + q + 2$$

the simplified versions are now

$$\begin{aligned}
 \bar{I}_0 = & \int_{r_1=0}^{\infty} \int_{r_2=0}^{\infty} r_2^{L_{\pi} + l} e^{-A_{\pi} r_2} r_1^{L_e - l - 1} e^{-A_e r_1} \\
 & \cdot {}_1F_1(l_{e_3} + 1 - i\eta; 2l_{e_3} + 2; 2ikr_1) dr_1 dr_2 \quad (3.21)
 \end{aligned}$$

3.3.2 Contribution to the Evaluation of Integrals Involving

$$I_1 = \int_{r_1=0}^{\infty} \int_{r_2=r_1}^{\infty} r_2^{L\pi+l} e^{-A\pi r_2} r_1^{L\pi-l-1} e^{-Ae r_1} \cdot {}_1F_1(l\epsilon_s + 1 - i\eta; 2l\epsilon_s + 2; 2ikr_1) dr_2 dr_1 \quad (3.22)$$

The integral to be considered

$$I_2 = \int_{r_1=0}^{\infty} \int_{r_2=r_1}^{\infty} r_2^{L\pi-l-1} e^{-A\pi r_2} r_1^{L\pi+l} e^{-Ae r_1} \quad (3.24)$$

where n is an integer, l is a positive real number, and γ are positive real numbers.

The most efficient method of evaluating these integrals is to first determine the value of the integral when $n = 2l$, and then use a three-term recurrence relation to calculate the integrals for the remaining values of n .

When $n = 2l$,

$$\begin{aligned} & \int_0^{\infty} y^l e^{-By} F_1(-x, y) dy \\ &= C_0(-x) \int_0^{\infty} y^{2l+1} e^{-(A+B)y} F_1(2l+1, x, 2l+2, 2iy) dy \\ &= C_0(-x) \frac{\Gamma(2l+2)}{(A+B)^{2l+2}} F_1(2l+1, x, 2l+2, \frac{2x}{A+B}) \\ &= C_0(-x) \Gamma(2l+2) \Gamma(1, B)^{-2l-2} \left(1 - \frac{2x}{A+B}\right)^{-2l-2} \quad (3.25) \\ &= C_0(-x) \Gamma(2l+2) (1/B^2)^{-2l-2} e^{-2x/B} \end{aligned}$$

The recurrence relation, which is easily derived using integration by parts and the differential equation

3.3.2 Introduction to the Evaluation of Integrals Involving Coulomb Wave Functions

The integral to be considered is

$$\int_0^{\infty} y^{m-l} e^{-By} F_l(-\gamma, y) dy \quad (3.24)$$

where m is an integer greater than or equal to -1 , and B and γ are positive real numbers.

The most efficient method of evaluating these integrals is to first determine the value of the integral when $m = 2l$, and then use a three-term recurrence relation to calculate the integrals for the remaining values of m .

When $m = 2l$,

$$\begin{aligned} & \int_0^{\infty} y^l e^{-By} F_l(-\gamma, y) dy \\ &= C_l(-\gamma) \int_0^{\infty} y^{2l+1} e^{-(i+B)y} {}_1F_1(l+1+i\gamma; 2l+2; 2iy) dy \\ &= C_l(-\gamma) \frac{\Gamma(2l+2)}{(i+B)^{2l+2}} {}_2F_1(l+1+i\gamma, 2l+2; 2l+2; \frac{2i}{i+B}) \\ &= C_l(-\gamma) \Gamma(2l+2) (i+B)^{-(2l+2)} \left(1 - \frac{2i}{i+B}\right)^{-(l+1+i\gamma)} \quad (3.25) \\ &= C_l(-\gamma) \Gamma(2l+2) (1+B^2)^{-(l+1)} e^{-2\gamma \cot^{-1} B} \end{aligned}$$

The recurrence relation, which is easily derived using integration by parts and the differential equation

has been evaluated. Normally two integrals would be required.

satisfied by the Coulomb Wave Function, is

$$\begin{aligned}
 (1+B^2) \int_0^{\infty} y^{m-l} e^{-By} F_l(-\gamma, y) dy \\
 = \left\{ 2(m-l)B - 2\gamma \right\} \int_0^{\infty} y^{m-l-1} e^{-By} F_l(-\gamma, y) dy \\
 + \left\{ l(l+1) - (m-l)(m-l-1) \right\} \int_0^{\infty} y^{m-l-2} e^{-By} F_l(-\gamma, y) dy \\
 + (2l+1) C_l \delta_{m,0}
 \end{aligned} \quad (3.26)$$

A similar recurrence relation can be derived from the properties of the ${}_2F_1$ function.

$$\begin{aligned}
 (1+B^2) \frac{\Gamma(m+2)}{(i+B)^{m+2}} {}_2F_1\left(m+2, l+1+\gamma; 2l+2; \frac{2i}{i+B}\right) \\
 = \left\{ 2(m-l)B - 2\gamma \right\} \frac{\Gamma(m+1)}{(i+B)^{m+1}} {}_2F_1\left(m+1, l+1+\gamma; 2l+2; \frac{2i}{i+B}\right) \\
 + (2l+1-m) \frac{\Gamma(m+1)}{(i+B)^m} {}_2F_1\left(m, l+1+\gamma; 2l+2; \frac{2i}{i+B}\right)
 \end{aligned} \quad (3.27)$$

However, caution should be used since for $m \leq 0$

$$\begin{aligned}
 \int_0^{\infty} y^{m-l-2} e^{-By} F_l(-\gamma, y) dy \\
 \neq C_l \frac{\Gamma(m)}{(i+B)^m} {}_2F_1\left(m, l+1+\gamma; 2l+2; \frac{2i}{i+B}\right)
 \end{aligned} \quad (3.28)$$

The question should now arise as to how a three term recurrence relation can be used when only one integral has been evaluated. Normally two integrals would be required.

For simplicity, denote

$$\frac{1}{C_l} \int_0^{\infty} y^{m-l} e^{-By} F_l(-\gamma, y) dy$$

by $G(m)$, then (3.26) can be written as

$$\begin{aligned} (1+B^2) G(m) &= 2[(m-l)B-\gamma] G(m-1) \\ &+ m(2l+1-m) G(m-2) \\ &+ (2l+1) \delta_{m,0} \end{aligned} \quad (3.29)$$

For $m = 0, 2l + 1$ (3.29) has only two terms.

$$\begin{aligned} (1+B^2) G(0) &= 2[-lB-\gamma] G(-1) + (2l+1) \\ (1+B^2) G(2l+1) &= 2[lB-\gamma] G(2l) \end{aligned} \quad (3.30)$$

These two (two-term) equations are sufficient to insure that all values of $G(m)$ can be evaluated from $G(2l)$.

Suppose M is the highest value of m for which it is desired to calculate $G(m)$, then the $M + 2$ simultaneous equations

$$\begin{aligned} (1+B^2) G(M) &= 2[(M-l)B-\gamma] G(M-1) + M(2l+1-M) G(M-2) \\ (1+B^2) G(M-1) &= \dots \\ &\vdots \\ (1+B^2) G(0) &= 2[-lB-\gamma] G(-1) + (2l+1) \end{aligned} \quad (3.31)$$

$$(1+B^2) G(0) = 2[-lB-\gamma] G(-1) + (2l+1)$$

$$G(2l) = \Gamma(2l+2) (1+B^2)^{-(l+1)} e^{-2\gamma \cos^{-1} B}$$

can be set up as a matrix equation (Chattarji 1976, p.45)

$$\begin{bmatrix}
 (1+B^2) & -2\{(M-\ell)B-\gamma\} & \dots & 0 \\
 0 & (1+B^2) & \dots & \\
 \vdots & \vdots & \ddots & \vdots \\
 0 & 0 & \dots & (1+B^2)
 \end{bmatrix}
 \begin{bmatrix}
 |G\rangle \\
 G(M) \\
 G(M-1) \\
 \vdots \\
 G(0) \\
 G(-1)
 \end{bmatrix}
 =
 \begin{bmatrix}
 |B\rangle \\
 0 \\
 0 \\
 \vdots \\
 (2\ell+1) \\
 G(2\ell)
 \end{bmatrix}
 \quad (3.32)$$

where the unit element in the last row of $[A]$ is in the $A_{M+1, M+1-2\ell}$ position.

This system of simultaneous equations can be solved directly on a computer by Gaussian elimination methods, which insure a high degree of accuracy by avoiding the truncation errors involved in series summation methods.

The fact that such simple techniques are available for the calculation of matrix elements may directly be ascribed to the symmetry properties of the Coulomb field.

There are complications, however, which arise when dealing with mesic atoms. When $m \leq 2\ell_{ef}$, $G(m) \sim B^{2\ell_{ef}-m-1}$, while for $m \geq 2\ell_{ef}$, $G(m) \sim B^{-m-2}$. For mesic atoms, $B \sim m_{\pi}/m_e$ and $B^{2\ell_{ef}+1}$ may be as large as $(273)^7 \approx 10^{16}$ (for octopole transitions in pionic helium).

One might be tempted to think that these terms dominate the final answer, but it turns out that all higher powers of B cancel identically when the sums over m are performed!!

It is necessary then to transform the usual expressions for these integrals so as to eliminate these terms.

It should also be noted that $G(m < 2\ell)$ is of the form $\alpha_1 e^{-2\gamma \cot^{-1} B} + \alpha_2$, while $G(m \geq 2\ell)$ is of the form $\beta e^{-2\gamma \cot^{-1} B}$. By separating the $G(m < 2\ell)$ into their component parts, like terms can be grouped and evaluated.

The Gauss' hypergeometric function is dependent on the relative values of $(L_0 - 1)$ and $(2\ell_{of} + 2)$. If $(L_0 - 1) > (2\ell_{of} + 2)$, then, using the transformation (A.20)

$$I_0' = \frac{\Gamma(L_0 + 1/2) \Gamma(L_0 - \ell)}{\Gamma(L_0 + 1/2 + \ell)} \left(\frac{A_c^*}{A_c} \right)^{-(L_0 + 1/2 - \ell)}$$

$${}_2F_1(L_0 + 1/2, (2\ell_{of} + 2) - (L_0 - \ell); 2\ell_{of} + 2; \frac{A_c^*}{A_c}) \quad (3.34)$$

where the Gauss' hypergeometric function is now a polynomial, and all terms contain the factor

$$\chi = e^{-2\gamma \cot^{-1} B} = \left(\frac{A_c^*}{A_c} \right)^{\gamma}$$

On the other hand, if $(2\ell_{of} + 2) > (L_0 - 1)$, the transformation (A.24) is used to obtain

3.3.3 Evaluation of $(I_0 - I_1)$. First Method

$$\begin{aligned}
 \bar{I}_0 &= \int_{r_1=0}^{\infty} \int_{r_2=0}^{\infty} r_1^{L_e-l-1} e^{-A_e r_1} {}_2F_1(l_{e3}+1-2\eta; 2l_{e3}+2; 2ikr_1) \\
 &\quad \cdot r_2^{L_\pi+l} e^{-A_\pi r_2} dr_2 dr_1 \\
 &= \frac{\Gamma(L_\pi+l+1)}{A_\pi^{L_\pi+l+1}} \frac{\Gamma(L_e-l)}{A_e^{L_e-l}} {}_2F_1(l_{e3}+1-2\eta, L_e-l; 2l_{e3}+2; \frac{2ik}{A_e}) \quad (3.33)
 \end{aligned}$$

The method for evaluation of the Gauss' hypergeometric function is dependent on the relative values of $(L_e - l)$ and $(2l_{ef} + 2)$. If $(L_e - l) \geq (2l_{ef} + 2)$, then, using the transformation (A.20)

$$\begin{aligned}
 \bar{I}'_0 &= \frac{\Gamma(L_\pi+l+1)}{A_\pi^{L_\pi+l+1}} \frac{\Gamma(L_e-l)}{A_e^{L_e-l}} \left(\frac{A_e^*}{A_e} \right)^{-(l_{e3}+1-2\eta)} \\
 &\quad {}_2F_1(l_{e3}+1-2\eta, (2l_{e3}+2)-(L_e-l); 2l_{e3}+2; \frac{-2ik}{A_e^*}) \quad (3.34)
 \end{aligned}$$

where the Gauss' hypergeometric function is now a polynomial, and all terms contain the factor

$$\chi \equiv e^{+2\eta \cot^{-1}(-\eta)} = \left(A_e^*/A_e \right)^{i\eta}$$

On the other hand, if $(2l_{ef} + 2) > (L_e - l)$, the transformation (A.24) is used to obtain

$$\begin{aligned}
I_0'' &= \frac{\Gamma(L_\pi + l + 1) \Gamma(l_e - l) \Gamma(2l_{e_s} + 2) \Gamma(-l_{e_s} - 1 - 2\eta + l_e - l)}{A_\pi^{L_\pi + l + 1} A_e^{l_e - l} \Gamma(l_{e_s} + 1 - 2\eta) \Gamma(l_e - l)} \\
&\cdot (A_e^* / A_e)^{(l_{e_s} + 1 + 2\eta - l_e + l)} (2ik / A_e)^{l_e - l - 2l_{e_s} - 2} \\
&\cdot {}_2F_1(2l_{e_s} + 2 - l_e + l, 1 - l_e + l; l_{e_s} + 2 + 2\eta - l_e + l; \frac{A_e^*}{-2ik}) \\
+ &\frac{\Gamma(L_\pi + l + 1) \Gamma(l_e - l) \Gamma(2l_{e_s} + 2) \Gamma(l_{e_s} + 1 + 2\eta - l_e + l)}{A_\pi^{L_\pi + l + 1} A_e^{l_e - l} \Gamma(l_{e_s} + 1 + 2\eta) \Gamma(2l_{e_s} + 2 - l_e + l)} \quad (3.35) \\
&\cdot (2ik / A_e)^{-l_e + l} {}_2F_1(l_e - l, l_e - l - 2l_{e_s} - 1; -l_{e_s} - 2\eta + l_e - l; \frac{A_e^*}{-2ik}) \\
&= I_{00}'' + I_{01}''
\end{aligned}$$

where I_{00}'' contains the factor χ and I_{01}'' does not.

Now $(L_e - l - 2l_{ef} - 1)$ is always a negative integer as is $(1 - L_e + l) = (l - l_{ei} - l_{ef}) - (s + 1)$. Therefore both hypergeometric functions are reduced to polynomials.

The second hypergeometric function will cancel with terms arising from the evaluation of I_1 and therefore no attempt will be made to simplify it further. I_{00}'' can be simplified by using the transformation (A.25).

$$\begin{aligned}
I_{00}'' &= \frac{\Gamma(L_\pi + l + 1) \Gamma(2l_{e_s} + 2) \Gamma(2l_{e_s} + 1) \Gamma(-l_{e_s} - 2\eta)}{A_\pi^{L_\pi + l + 1} \Gamma(2l_{e_s} + 2 - l_e + l) \Gamma(l_{e_s} + 1 - 2\eta)} \\
&\cdot \frac{(-1)^{l_e - l - 1} \chi}{(2ik)^{2l_{e_s} + 1}} A_e^{l_{e_s} + 1 - l_e + l} A_e^*^{l_{e_s}} \\
&\cdot {}_2F_1(1 - l_e + l, -l_{e_s} - 2\eta; -2l_{e_s}; \frac{-2ik}{A_e^*}) \quad (3.36)
\end{aligned}$$

$$\begin{aligned}
I_1 &= \int_{r_1=0}^{\infty} r_1^{L_e - l - 1} e^{-A_e r_1} {}_1F_1(l_{ef} + 1 - 2\eta; 2l_{ef} + 2; 2ikr_1) \\
&\quad \cdot \int_{r_2=r_1}^{\infty} r_2^{L_\pi + l} e^{-A_\pi r_2} dr_2 dr_1 \\
&= \frac{\Gamma(L_\pi + l + 1)}{A_\pi^{L_\pi + l + 1}} \sum_{z=0}^{L_\pi + l} \frac{A_\pi^z}{z!} \frac{\Gamma(L_e - l + z)}{(A_\pi + A_e)^{L_e - l + z}} \\
&\quad \cdot {}_2F_1(l_{ef} + 1 - 2\eta, L_e - l + z; 2l_{ef} + 2; \frac{2ik}{A_\pi + A_e})
\end{aligned} \tag{3.37}$$

Again if $(L_e - l) \geq (2l_{ef} + 2)$, transformation (A.20) is used to evaluate I_1

$$\begin{aligned}
I_1' &= \frac{\Gamma(L_\pi + l + 1)}{A_\pi^{L_\pi + l + 1}} \sum_{z'=L_e - l - (2l_{ef} + 2)}^{L_\pi + l - (2l_{ef} + 2)} \frac{A_\pi^{z' + 2l_{ef} + 2 - L_e + l}}{(A_\pi + A_e)^{2l_{ef} + 2 + z'}} \\
&\quad \cdot \frac{\Gamma(2l_{ef} + 2 + z')}{\Gamma(z' + 2l_{ef} + 3 - L_e + l)} \left(\frac{A_\pi + A_e^*}{A_\pi + A_e} \right)^{-(l_{ef} + 1 - \eta)} \\
&\quad \cdot {}_2F_1(l_{ef} + 1 - 2\eta, -z'; 2l_{ef} + 2; \frac{-2ik}{A_\pi + A_e^*})
\end{aligned} \tag{3.38}$$

where all terms contain the factor

$$\Psi \equiv \left(\frac{A_\pi + A_e^*}{A_\pi + A_e} \right)^{z'}$$

However, if $(2l_{ef} + 2) > (L_e - l)$, the series must be divided into two subseries, one with $t \leq (2l_{ef} + 1) - (L_e - l)$ and the other where $t \geq (2l_{ef} + 2) - (L_e - l)$. Hence

$$\begin{aligned}
I_1'' &= \frac{\Gamma(L_\pi + l + 1)}{A_\pi^{L_\pi + l + 1}} \sum_{z=0}^{(2l_{e3} + 1) - (L_e - l)} \frac{A_\pi^z \Gamma(L_e - l + z)}{z! (A_\pi + A_e)^{L_e - l + z}} \\
&\quad \cdot {}_2F_1(l_{e3} + 1 - iz, L_e - l + z; 2l_{e3} + 2; \frac{2ik}{A_\pi + A_e}) \\
&+ \frac{\Gamma(L_\pi + l + 1)}{A_\pi^{L_\pi + l + 1}} \sum_{z'=0}^{L_e + l - (2l_{e3} + 2)} \frac{A_\pi^{z' + (2l_{e3} + 2) - (L_e - l)}}{(A_\pi + A_e)^{z' + 2l_{e3} + 2}} \\
&\quad \cdot \frac{\Gamma(z' + 2l_{e3} + 2)}{\Gamma(z' + 2l_{e3} + 3 - L_e + l)} {}_2F_1(l_{e3} + 1 - iz', z' + 2l_{e3} + 2; 2l_{e3} + 2; \frac{2ik}{A_\pi + A_e}) \\
&= I_{10}'' + I_{11}''
\end{aligned} \tag{3.39}$$

where all the terms of I_{11}'' contain the factor χ , but where the terms of I_{10}'' are mixed.

For the second set of terms, the transformation (A.20) can be used to reduce each hypergeometric function to a polynomial.

At this point if all terms of I_0 and I_1 were evaluated and arranged in descending powers of A_π (which is proportional to $M = m_\pi/m_e$), the highest power of A_π in I_0 would be $(-L_\pi - l - 1)$. For I_{10}'' it would be $(-L_\pi - L_e + 2l_{ef})$, while for I_{11}'' and I_1' , it would be $(-L_\pi - L_e - 1)$.

Now $(-L_\pi - l - 1) > (-L_\pi - L_e - 1)$ since $l_{ei} + l_{ef} + s + 2 = L_e$. Therefore it might be expected that $I_0 > I_{11}''$ or I_1' .

However, when $(2l_{ef} + 2) > (L_e - l)$, $(-L_\pi - L_e + 2l_{ef}) \geq (-L_\pi - l - 1)$ or $I_{10}'' \geq I_0$.

For example, if $(n_{ei}, l_{ei}) = (1, 0)$, $l_{ef} = l$, then

$$I_{10}'' \sim M^{+l-2}$$

$$I_0 \sim M^{-l-1}$$

$$I_{11}'' \sim M^{-l-3} \quad (3.41)$$

It would be most unusual indeed if the major contribution to the total integral came from the penetration terms. The author therefore suspected (and confirmed) that upon summation over t , all higher orders of A_π in I_{10}'' vanished identically.

As in the evaluation of I_0'' , transformation (A.24) is used to separate the terms which contain the factor Ψ from those which do not.

$$\begin{aligned} I_{10}'' &= \frac{\Gamma(L_\pi + l + 1) \Gamma(l_e - l) \Gamma(2l_{e_g} + 2) \Gamma(l_{e_g} + 1 + i\eta - l_e + l)}{A_\pi^{L_\pi + l + 1} (2ik)^{l_e - l} \Gamma(2l_{e_g} + 2 - l_e + l) \Gamma(l_{e_g} + 1 + i\eta)} \\ &\cdot \sum_{z=0}^{2l_{e_g} + 1 - l_e + l} \left(\frac{A_\pi}{2ik} \right)^z \frac{(l_e - l)_z (-2l_{e_g} - 1 + l_e - l)_z}{(-l_{e_g} - i\eta + l_e - l)_z z!} \\ &\cdot {}_2F_1(l_e - l + z, l_e - l - 2l_{e_g} - 1 + z; -l_{e_g} - i\eta + l_e - l + z; \frac{A_\pi + A_e}{-2ik}) \\ &+ \frac{\Gamma(L_\pi + l + 1) \Gamma(2l_{e_g} + 2) |A_\pi + A_e|^{2(l_{e_g} + 1 - l_e + l)} \Psi}{A_\pi^{L_\pi + l + 1} \Gamma(l_{e_g} + 1 - i\eta) (2ik)^{2l_{e_g} + 2 + l - l_e}} \\ &\cdot \sum_{z=0}^{2l_{e_g} + 1 - l_e + l} \left[\frac{2ik A_\pi}{|A_\pi + A_e|^2} \right]^z \frac{\Gamma(-l_{e_g} - 1 - i\eta + l_e - l + z)}{z!} \\ &\cdot {}_2F_1(-l_e + l + 2l_{e_g} + 2 - z, 1 - l_e + l - z; l_{e_g} + 2 + i\eta - l_e + l - z; \frac{A_\pi + A_e}{-2ik}) \end{aligned} \quad (3.40)$$

$$I_{10}'' = I_{100}'' + I_{101}''$$

I_{100}'' is merely a Taylor series and reduces to

$$\frac{\Gamma(L\pi + l + 1) \Gamma(2l e_s + 2) \Gamma(l e - l) \Gamma(l e_s + 1 + 2\eta - l e + l)}{A_\pi^{L\pi + l + 1} \Gamma(l e_s + 1 + 2\eta) \Gamma(2l e_s + 2 - l e + l)} \quad (3.41)$$

$$\cdot {}_2F_1(l e - l, l e - l - 2l e_s - 1; -l e_s - 2\eta + l e - l; A e^* / -2ik)$$

which is identically I_{01}'' . Therefore I_{100}'' and I_{01}'' do not appear in the final answer.

At this point all remaining terms contain either the factor χ or the factor Ψ .

To evaluate I_{101}'' , first reverse the order of summation, then use the identity

$$\begin{aligned} \sum_{z=0}^{2l-N} \binom{N-2l}{(d)_z} z^z {}_2F_1(1+z, -2l+z; d+z; y) \\ = \sum_{z=0}^N \binom{-N}{(d)_z} (-z)^z {}_2F_1(1+z, -2l+z; d+z; z+y) \end{aligned} \quad (3.42)$$

which can be proved by expanding the hypergeometric function in a Taylor series and rearranging terms.

This rearrangement successfully eliminates the higher powers of A_π such that

$$I_{101}'' = \frac{\Gamma(L_\pi + l + 1) \Gamma(2l_{ef} + 2) \Gamma(l_{ef} - 2\eta) A_\pi^{2l_{ef} + 1 - L_e + l} \psi}{A_\pi^{L_\pi + l + 1} \Gamma(2l_{ef} + 2 - L_e + l) \Gamma(l_{ef} + 1 - 2\eta) (2ik) |A_\pi + Ae|^{2l_{ef}}}$$

$$\cdot \sum_{k=0}^{l_{ef}-l-1} \frac{(1+l-L_e)_k}{(1-l_{ef}+2\eta)_k} \left[\frac{|A_\pi + Ae|^2}{-2ikA_\pi} \right]^k \quad (3.43)$$

$$\cdot {}_2F_1(1+K, -2l_{ef}+K; -l_{ef}+1+2\eta+k; \frac{Ae(A_\pi + Ae^*)}{2ikA_\pi})$$

with the highest order of A_π being $(-L_\pi - l - 1)$ and no longer $(-L_\pi - L_e + 2l_{ef})$.

$$\frac{\Gamma(b)}{\Gamma(b)} \left[1 - e^{-sy} \sum_{z=0}^{b-1} \frac{(sy)^z}{z!} \right] \quad (3.44)$$

is used.

However, there is an alternate form, which, while first appearing more complicated, simplifies the evaluation of $I_0'' - I_1''$.

$$\int_0^y x^{b-1} e^{-sx} dx = e^{-sy} y^b \sum_{z=0}^{\infty} \frac{(sy)^z \Gamma(b)}{\Gamma(b+z+1)} \quad (3.45)$$

Hence

$$(I_0 - I_1)'' = \Gamma(L_\pi + l + 1) \sum_{z=0}^{\infty} \frac{A_\pi^z \Gamma(L_e + L_\pi + 1 + z)}{\Gamma(L_\pi + l + 2 + z)} \quad (3.46)$$

$$\cdot (A_\pi + Ae)^{-(L_e + L_\pi + 1 + z)}$$

$$\cdot {}_2F_1(L_\pi + l + 2\eta, L_e + L_\pi + 1 + z, 2l_{ef} + 2, \frac{2ik}{A_\pi + Ae})$$

3.3.4 Evaluation of $(I_0'' - I_1'')$. Second Method.

At this point it is appropriate to ask whether there is an alternate way of evaluating $(I_0'' - I_1'')$ which avoids both those terms lacking in the factors χ and Ψ , and those terms containing the higher powers of A_π .

Usually when the integral

$$\int_0^y x^{b-1} e^{-sx} dx$$

where b is an integer, is evaluated, the form

$$\frac{\Gamma(b)}{s^b} \left[1 - e^{-sy} \sum_{z=0}^{b-1} \frac{(sy)^z}{z!} \right] \quad (3.44)$$

is used.

However, there is an alternate form, which, while first appearing more complicated, simplifies the evaluation of $I_0'' - I_1''$.

$$\int_0^y x^{b-1} e^{-sx} dx = e^{-sy} y^b \sum_{z=0}^{\infty} \frac{(sy)^z \Gamma(b)}{\Gamma(b+z+1)} \quad (3.45)$$

Hence

$$(I_0 - I_1)'' = \Gamma(l\pi + l + 1) \sum_{z=0}^{\infty} \frac{A_\pi^z \Gamma(l\pi + l + 1 + z)}{\Gamma(l\pi + l + 2 + z)} \quad (3.46)$$

$$- (A_\pi + Ae)^{-(l\pi + l + 1 + z)}$$

$$\cdot {}_2F_1(l\pi + l + 1, l\pi + l + 1 + z; 2l\pi + 2; \frac{2ik}{A_\pi + Ae})$$

Now since $L_e + L_\pi - 2l_{ef} - 1 > 0$, define

$t' = t + (L_e + L_\pi - 2l_{ef} - 1)$ and hence

$$(\bar{I}_0 - I_1)'' = \frac{\Gamma(L_\pi + l + 1) A_\pi^{2l_{ef} + 1 - l_e - L_\pi}}{(A_\pi + A_e)^{2l_{ef} + 2}} \sum_{z = l_e + L_\pi - 2l_{ef} - 1}^{\infty} \left(\frac{A_\pi}{A_\pi + A_e} \right)^z \quad (3.47)$$

$$\cdot \frac{\Gamma(2l_{ef} + 2 + z)}{\Gamma(2l_{ef} + 3 + z + l - l_e + z)} {}_2F_1(l_{ef} + 1 - 2\eta, 2l_{ef} + 2 + z; 2l_{ef} + 2; \frac{2ik}{A_\pi + A_e})$$

or, by adding I_{11}'' to both sides of the above and using (A.20) to reduce each hypergeometric function to a polynomial

$$(\bar{I}_0 - I_1)'' + I_{11}'' = \frac{\Gamma(L_\pi + l + 1) \Psi A_\pi^{2l_{ef} + 1 - l_e - L_\pi}}{|A_\pi + A_e|^{2l_{ef} + 2}} \sum_{z=0}^{\infty} \left(\frac{A_\pi}{A_\pi + A_e} \right)^z \quad (3.48)$$

$$\cdot \frac{\Gamma(2l_{ef} + 2 + z)}{\Gamma(2l_{ef} + 3 + l - l_e + z)} {}_2F_1(l_{ef} + 1 - 2\eta, -z; 2l_{ef} + 2; \frac{-2ik}{A_\pi + A_e^*})$$

Now use Vandermonde's theorem to expand

$$\frac{\Gamma(2l_{ef} + 2 + z)}{\Gamma(2l_{ef} + 3 + l - l_e + z)} = \sum_{k=0}^{l_e - l - 1} \frac{(l_e - l - 1)! (2l_{ef} - k)!}{(l_e - l - 1 - k)! (2l_{ef} - l_e + l + 1)!} \frac{(k+1)z}{z!} \quad (3.49)$$

and the sum formula (A.30), to obtain

$$(\bar{I}_0 - I_1)'' + I_{11}'' = \frac{\Gamma(L_\pi + l + 1) A_\pi^{2l_{ef} + 1 - l_e - L_\pi} \Psi}{|A_\pi + A_e|^{2l_{ef} + 2}} \left(\frac{A_\pi + A_e}{A_e} \right) \sum_{k=0}^{l_e - l - 1} \left(\frac{A_\pi + A_e}{A_e} \right)^k \quad (3.50)$$

$$\cdot \frac{(l_e - l - 1)! (2l_{ef} - k)!}{(l_e - l - 1 - k)! (2l_{ef} - l_e + l + 1)!} {}_2F_1(k+1, l_{ef} + 1 - 2\eta; 2l_{ef} + 2; \frac{2ik A_\pi}{A_e (A_\pi + A_e^*)})$$

Now the transformation (A.22) is used to separate the terms containing χ from those containing Ψ .

$$\begin{aligned}
 & (I_0 - I_1)'' + I_1'' \\
 &= \frac{\Gamma(L_\pi + l + 1) \Psi \Gamma(2l_{eS} + 2) \Gamma(l_{eS} - 2\eta) A_\pi^{2l_{eS} + 1 - l_e - L_\pi}}{|A_\pi + A_e|^{2l_{eS} + 2} \Gamma(2l_{eS} + 2 - l_e + l) \Gamma(l_{eS} + 1 - 2\eta)} \\
 & \cdot \sum_{k=0}^{l_e - l - 1} \left[\frac{|A_\pi + A_e|^2}{-2ik A_\pi} \right]^{k+1} \frac{(1 + l - l_e)_k}{(1 - l_{eS} + i\eta)_k} \\
 & \cdot {}_2F_1 \left(1 + k, -2l_{eS} + k; 1 - l_{eS} + 2\eta + k; \frac{A_e (A_\pi + A_e^*)}{2ik A_\pi} \right) \\
 & + \frac{\Gamma(L_\pi + l + 1) \Gamma(2l_{eS} + 2) \Gamma(2l_{eS} + 1) \Gamma(-l_{eS} + i\eta) \Psi}{\Gamma(2l_{eS} + 2 - l_e + l) \Gamma(l_{eS} + 1 + 2\eta) |A_\pi + A_e|^{2l_{eS} + 2}} \\
 & \cdot A_\pi^{2l_{eS} + 1 - l_e - L_\pi} \left(\frac{-2ik A_\pi}{A_e (A_\pi + A_e^*)} \right)^{-l_{eS} - 1 + i\eta} \\
 & \cdot \sum_{k=0}^{l_e - l - 1} \frac{(1 + l - l_e)_k}{(-2l_{eS})_k} \frac{(-l_{eS} + 2i\eta)_k}{k!} \left(\frac{A_\pi + A_e}{A_e} \right)^{k+1} \\
 & \cdot {}_2F_1 \left(l_{eS} + 1 - 2\eta, -l_{eS} - 2\eta; l_{eS} + 1 - 2\eta - k; \frac{A_e (A_\pi + A_e^*)}{2ik A_\pi} \right)
 \end{aligned} \tag{3.51}$$

where the first set of terms is easily recognized as $-I_{101}''$, and I_{01}'' can be retrieved from the second set by using the summation formula (A31) and taking the complex conjugate of the result.

3.3.5 Summary

I_2 is easily evaluated and is simply

$$I_2 = \frac{\Gamma(L_\pi - l) A_\pi^{2l_\pi + 1 - L_\pi - L_e} \Psi}{|A_\pi + A_e|^{2l_\pi + 2}} \sum_{z = l_e + l - 2l_\pi - 1}^{l_e + L_\pi - 2l_\pi - 2} \left(\frac{A_\pi}{A_\pi + A_e} \right)^z \quad (3.52)$$

$$\frac{\Gamma(2l_\pi + 2 + z)}{\Gamma(2l_\pi + 2 - l_e - l + z)} {}_2F_1(l_\pi + 1 - i\eta, -z; 2l_\pi + 2; \frac{-2ik}{A_\pi + A_e^*})$$

Gathering I_0 , I_1 , and I_2 together, the total integral I can be written as

$$I' = \frac{\Gamma(L_\pi + l + 1) \Gamma(L_e - l)}{A_\pi^{L_\pi + l + 1} A_e^{L_e - l}} \left(\frac{A_e^*}{A_e} \right)^{-(l_\pi + 1 - i\eta)} \cdot {}_2F_1(l_\pi + 1 - i\eta, 2l_\pi + 2 - l_e + l; 2l_\pi + 2; \frac{-2ik}{A_e^*})$$

$$- \frac{\Psi A_\pi^{2l_\pi + 1 - l_e - L_\pi}}{|A_\pi + A_e|^{2l_\pi + 2}} \sum_{z=0}^{L_\pi + l_e - 2l_\pi - 2} \left(\frac{A_\pi}{A_\pi + A_e} \right)^z \Gamma(2l_\pi + 2 + z) \quad (3.53)$$

$$\cdot \left[\frac{\Gamma(L_\pi + l + 1)}{\Gamma(2l_\pi + 2 - l_e + l + z)} - \frac{\Gamma(L_\pi - l)}{\Gamma(2l_\pi + 2 - l_e - l + z)} \right] {}_2F_1(l_\pi + 1 - i\eta, -z; 2l_\pi + 2; \frac{-2ik}{A_\pi + A_e^*})$$

when $(L_e - l) \geq (2l_{ef} + 2)$; and as

$$I'' = \frac{\Gamma(L_\pi + l + 1) \Gamma(2l_\pi + 2) \Gamma(2l_\pi + 1) \Gamma(-l_\pi - i\eta) (-1)^{L_e - l - 1} \chi(A_e^*)^{l_\pi}}{A_\pi^{L_\pi + l + 1} \Gamma(2l_\pi + 2 - l_e + l) \Gamma(l_\pi + 1 - i\eta) (2ik)^{2l_\pi + 1} A_e^{l_e - l - l_\pi - 1}}$$

$$\cdot {}_2F_1(1 - l_e + l, -l_\pi - i\eta; -2l_\pi; \frac{-2ik}{A_e^*})$$

+

Now by using one of the relations among contiguous

$$\begin{aligned}
& - \frac{\Gamma(L_{\pi} + l + 1) \Psi \Gamma(2l_{ef} + 2) \Gamma(l_{ef} - 2i\eta) A_{\pi}^{2l_{ef} + 1 - L_e + l}}{A_{\pi}^{L_{\pi} + l + 1} \Gamma(2l_{ef} + 2 - l_e + l) \Gamma(l_{ef} + 1 - 2i\eta) (2ik) |A_{\pi} + A_e|^{2l_{ef}}} \\
& \cdot \sum_{d=0}^{l_e - l - 1} \frac{(l + l - l_e)_d}{(1 - l_{ef} + 2i\eta)_d} \left[\frac{|A_{\pi} + A_e|^2}{-2ik A_{\pi}} \right]^d {}_2F_1(1 + d, -2l_{ef} + d; -l_{ef} + 1 + 2i\eta + d; \frac{A_e(A_{\pi} + A_e^*)}{2ik A_{\pi}}) \\
& - \frac{\Psi A_{\pi}^{2l_{ef} + 1 - l_e - L_{\pi}}}{|A_{\pi} + A_e|^{2l_{ef} + 2}} \sum_{z=0}^{L_{\pi} + l_e - 2l_{ef} - 2} \left(\frac{A_{\pi}}{A_{\pi} + A_e} \right)^z \Gamma(2l_{ef} + 2 + z) \quad (3.54) \\
& \cdot \left[\frac{\Gamma(L_{\pi} + l + 1)}{\Gamma(2l_{ef} + 3 - l_e + l + z)} - \frac{\Gamma(L_{\pi} - l)}{\Gamma(2l_{ef} + 2 - l_e - l + z)} \right] {}_2F_1(l_{ef} + 1 - 2i\eta, -z; 2l_{ef} + 2; \frac{-2ik}{A_{\pi} + A_e^*})
\end{aligned}$$

when $(2l_{ef} + 2) > (L_e - l)$.

Now the terms $(I_{11} - I_2)$ appear in both I' and I'' and can be simplified for mesic atoms in the following manner.

First define

$$H(t) = \left(\frac{A_{\pi}}{A_{\pi} + A_e} \right)^t {}_2F_1(l_{ef} + 1 - 2i\eta, -t; 2l_{ef} + 2; \frac{-2ik}{A_{\pi} + A_e^*}) \quad (3.55)$$

then

$$\begin{aligned}
I_{11} - I_2 & = \frac{\Psi A_{\pi}^{2l_{ef} + 1 - l_e - L_{\pi}}}{|A_{\pi} + A_e|^{2l_{ef} + 2}} \sum_{z=0}^{L_{\pi} + l_e - 2l_{ef} - 2} \Gamma(2l_{ef} + 2 + z) \\
& \cdot \left[\frac{\Gamma(L_{\pi} + l + 1)}{\Gamma(2l_{ef} + 3 - l_e + l + z)} - \frac{\Gamma(L_{\pi} - l)}{\Gamma(2l_{ef} + 2 - l_e - l + z)} \right] H(z) \quad (3.56)
\end{aligned}$$

Now by using one of the relations among contiguous

hypergeometric functions, a recurrence relation for the $H(t)$'s is obtained.

$$\begin{aligned}
 & (2l_{eS} + 2 + z) |A_{\pi} + A_e|^2 H(z+1) \\
 & - 2 \left[(z + l_{eS} + 1) A_{\pi}^2 + (z + l_{eS}) \frac{z_c}{a_0} A_{\pi} \right] H(z) \\
 & + z A_{\pi}^2 H(z-1) = 0
 \end{aligned} \tag{3.57}$$

The first few values of $H(t)$ are

$$H(0) = 1$$

$$H(1) = \frac{(2l_{eS} + 2) A_{\pi}^2 + (2l_{eS}) A_{\pi} \frac{z_c}{a_0}}{(2l_{eS} + 2) |A_{\pi} + A_e|^2}$$

$$\begin{aligned}
 H(2) = & \frac{(2l_{eS} + 2)(2l_{eS} + 3) A_{\pi}^4 + 4 l_{eS} (2l_{eS} + 3) A_{\pi}^3 \frac{z_c}{a_0} \\
 & + (2l_{eS} + 2)(2l_{eS} - 1) A_{\pi}^2 \left(\frac{z_c}{a_0}\right)^2 + (2l_{eS} + 2) A_{\pi}^2 K^2}{(2l_{eS} + 2)(2l_{eS} + 3) |A_{\pi} + A_e|^4} \\
 & \dots
 \end{aligned} \tag{3.58}$$

The expressions for $H(t)$ become increasingly more complicated, however since A_{π} is proportional to M , which is usually a large number, an approximate value for $H(t)$ may be found by keeping only the highest power of A_{π} . If this is done then $H(t)$ is approximately 1 for all t . While this is usually an excellent approximation (within 1% for most transitions), its inaccuracy increases as L_{π} increases. Therefore it would be wise to include the next lower power of A_{π} , hence

3.3.6 Simplification in the Case of Helium

$$H(z) \approx 1 - \left(\frac{Z_c}{a_0 A_\pi} \right) \frac{(2l_{e3} + 4)}{(2l_{e3} + 2)} z \quad (3.59)$$

Now by writing

$$1 - \left(\frac{Z_c}{a_0 A_\pi} \right) \frac{(2l_{e3} + 4)}{(2l_{e3} + 2)} z$$

as

$$\left[1 + \frac{Z_c}{a_0 A_\pi} (2l_{e3} + 4) \right] - \left[\frac{Z_c}{a_0 A_\pi} \frac{(2l_{e3} + 4)}{(2l_{e3} + 2)} (2l_{e3} + 2 + z) \right] \quad (3.60)$$

and using the sum formula (A.28), the sums can be evaluated and hence

$$I_{II} - I_2 \approx A_\pi \frac{2l_{e3} + 1 - l_c - l_\pi}{|A_\pi + A_e|^{2l_{e3} + 2}} \psi$$

$$\cdot \left\{ \Gamma(l_\pi + l_c + 1) \left[1 + \frac{Z_c}{a_0 A_\pi} (2l_{e3} + 4) \right] \frac{(2l + 1)}{(l_c - l)(l_c + l + 2)} \right.$$

$$- \frac{\Gamma(l_\pi + l_c + 2) \frac{Z_c}{a_0 A_\pi} (2l_{e3} + 4)}{a_0 A_\pi (2l_{e3} + 2)} \frac{(2l + 1)}{(l_c - l + 1)(l_c + l + 2)} \quad (3.61)$$

$$- \frac{\Gamma(l_\pi + l + 1) \Gamma(2l_{e3} + 2) \left[(l_c - l + 1) + \left(\frac{Z_c}{a_0 A_\pi} \right) (2l_{e3} + 4) \right]}{\Gamma(2l_{e3} + 2 - l_c + l) (l_c - l)(l_c - l + 1)}$$

$$+ \left. \frac{\Gamma(l_\pi - l) \Gamma(2l_{e3} + 2) \left[(l_c + l + 2) + \left(\frac{Z_c}{a_0 A_\pi} \right) (2l_{e3} + 4) \right]}{\Gamma(2l_{e3} + 1 - l_c - l) (l_c + l + 1)(l_c + l + 2)} \right\}$$

Now $P(-1)$ and $P(2l_{e3})$ are easily calculated, yielding

3.3.6 Simplification in the Case of Helium

Fortunately, the actual evaluation of these terms is easier than may first appear. In the case of mesic helium, $\ell_{ei} = 0$, $\ell_{ef} = \ell$ and $L_e = \ell + 2$, therefore

$$I_{0\ell}'' = \frac{K^{-2} \Gamma(L_{\pi} + \ell + 1) \Gamma(2\ell + 2) (\ell + 1) \chi (1 + \eta^2)^{\ell - 1}}{A_{\pi}^{L_{\pi} + \ell + 1} (\ell^2 + \eta^2) (\ell - 1)^2 + \eta^2 \dots (1 + \eta^2) 2^{2\ell}} \quad (3.62)$$

or by defining $B = 1 + 1/\eta^2$

$$I_{0\ell}'' = \left(\frac{a_0}{Zc}\right)^2 \frac{\Gamma(L_{\pi} + \ell + 1) \Gamma(2\ell + 2) (\ell + 1) \chi B^{\ell - 1}}{A_{\pi}^{L_{\pi} + \ell + 1} (\ell^2 B - \ell^2 + 1) \dots (B) 2^{2\ell}} \quad (3.63)$$

where again $\chi = e^{+2\eta \cot^{-1}(\eta)}$.

To evaluate $I_{10\ell}''$, first define

$$P(d) = \frac{1}{(2i)(\ell_{\pi} - i\eta)} \frac{1}{(1 - \ell_{\pi} + i\eta)_d} \left[\frac{|A_{\pi} + A_e|^2}{-2ikA_{\pi}} \right]^d \quad (3.64)$$

$$= {}_2F_1(1+d, -2\ell_{\pi} + d; -\ell_{\pi} + 1 + i\eta + d; \frac{A_{\pi}(A_{\pi} + A_e^*)}{2ikA_{\pi}})$$

then use the hypergeometric differential equation (A.19) to obtain the recurrence relation

$$\begin{aligned} |A_e|^2 (d+2)(1 - 2\ell_{\pi} + d) P(d+2) \\ = 2 \left[A_{\pi} \frac{Zc}{a_0} (d - \ell_{\pi}) + |A_e|^2 (1 + d - \ell_{\pi}) \right] P(d+1) \\ - |A_{\pi} + A_e|^2 P(d) \end{aligned} \quad (3.65)$$

Now $P(-1)$ and $P(2\ell_{ef})$ are easily calculated, yielding

$$P(-1) = \frac{K A_{\pi}}{|A_{\pi} + A_e|^2} \quad (3.66)$$

$$P(2\ell_{ef}) = \frac{1}{2\eta} \left[\frac{|A_{\pi} + A_e|^2}{2K A_{\pi}} \right]^{2\ell_{ef}} \frac{1}{(\ell_{ef}^2 + \eta^2) \dots (1 + \eta^2)}$$

By using the recurrence relation $2\ell_{ef}$ times, and the two above values of $P(-1)$ and $P(2\ell_{ef})$, a system of $2\ell_{ef}$ linear equations in $2\ell_{ef}$ unknowns -- $P(0)$ through $P(2\ell_{ef} - 1)$, is obtained. Consequently for all values of d , $P(d)$ can be calculated quickly on an electronic computer by Gaussian elimination.

Alternately, when the Auger electron is in the ground state $L_e - \ell - 1 = 1$ and only $P(0)$ and $P(1)$ are needed. In this case I_{101} is simply

$$I_{101} = - \frac{K^{-2} \Gamma(L_{\pi} + \ell + 1) \Psi \Gamma(2\ell + 2)}{A_{\pi}^{L_{\pi} + \ell + 1} \Gamma(2\ell + 1) |1 + A_e/A_{\pi}|^{2\ell} (1 + \eta^2)} J(\ell) \quad (3.67)$$

where

$$J(\ell) = 1 + \frac{(\ell + 1)(-\eta)}{(i\ell + \eta)} {}_2F_1(-2\ell, 1; -\ell + 1 + 2\eta; \frac{A_e(A_{\pi} + A_e^*)}{2iK A_{\pi}})$$

By using the relations for contiguous hypergeometric functions, a two-term recurrence relation can be found for $J(\ell)$.

$$\frac{2[(l+1)^2 B - l^2 - 2l] J(l+1)}{(2l+1)(l+2) B} \quad (3.68)$$

$$= J(l) - [l + (2l)(l+2)D + (2l+1)(l+2) B D^2] / (2l+1)(l+2) Q^{l+1}$$

where $B = 1 + 1/\eta^2$

$$D = Z_e / (a_0 A_\pi)$$

$$Q = 1 + 2D + BD^2$$

The first few values of $J(l)$ are

$$J(0) = 0$$

$$J(1) = -BD^2 Q^{-1} \quad (3.69)$$

$$J(2) = \frac{-B(1 + 6D + 18BD^2 + 18BD^3 + 9B^2D^4)}{2(4B - 3) Q^2}$$

....

I_{101}'' can then be concisely written as

$$I_{101}'' = - \left(\frac{a_0}{Z_e} \right)^2 \frac{\Gamma(L_\pi + l + 1) \Psi \Gamma(2l + 2) J(l)}{A_\pi^{L_\pi + l + 1} \Gamma(2l + 1) Q^l B} \quad (3.70)$$

Similarly for helium, $I_{111}'' - I_2$ simplifies to

$$\begin{aligned} I_{111}'' - I_2 &= \frac{\Psi}{Q^{l+1}} \left\{ \frac{(2l+1) \Gamma(L_\pi + l + 3)}{2(2l+3) A_\pi^{L_\pi + l + 3}} - \frac{(2l+1)(2l) \Gamma(L_\pi + l + 1)}{2 A_\pi^2 A_\pi^{L_\pi + l + 1}} \right\} \\ &+ \left(\frac{Z_e}{a_0} \right) \frac{\Psi}{Q^{l+1}} \left\{ \frac{(2l+4)(2l+1) \Gamma(L_\pi + l + 3)}{2(2l+3) A_\pi A_\pi^{L_\pi + l + 3}} \right. \\ &\left. - \frac{(2l+1) \Gamma(L_\pi + l + 4)}{(2l+2) 3 A_\pi^{L_\pi + l + 4}} - \frac{(2l+4)(2l+1)(2l) \Gamma(L_\pi + l + 1)}{6 A_\pi^3 A_\pi^{L_\pi + l + 1}} \right\} \end{aligned} \quad (3.71)$$

CHAPTER 4

THE PRESENT WORK. FORMULAE4.1 The General Formula

The most general version of the transition rate formula is

$$\omega_{i \rightarrow f} = \frac{1}{(2\pi)^2} \frac{1}{\hbar} \left(\frac{e^2}{a_0} \right) K \sum_{l_{e_1}, l} \frac{(2l_{e_1} + 1)}{(2l + 1)} \begin{pmatrix} l & l_{e_1} & l_{e_2} \\ 0 & 0 & 0 \end{pmatrix}^2 \quad (4.1)$$

$$\cdot \frac{(2l_{e_2} + 1)}{(2l + 1)} \begin{pmatrix} l & l_{e_2} & l_{e_3} \\ 0 & 0 & 0 \end{pmatrix}^2 \left| R_{l_{e_1}, l} \right|^2$$

where

$$R_{l_{e_1}, l} = 4\pi (-i)^{l_{e_2}} e^{-i\sigma_{l_{e_2}}} C_{l_{e_2}}^{(l)}(\eta) k^{l_{e_2}}$$

$$\cdot \left(\frac{Ze}{a_0} \right)^{3/2} \frac{2}{n_{e_2}^2} \sum_{s=0}^{n_{e_2} - l_{e_2} - 1} (-1)^s \frac{[(n_{e_2} + l_{e_2})! (n_{e_2} - l_{e_2} - 1)!]^{1/2}}{(n_{e_2} - l_{e_2} - 1 - s)! s! (2l_{e_2} + 1 + s)!} \left(\frac{2Zc}{n_{e_2} a_0} \right)^{l_{e_2} + s}$$

$$\cdot \left(\frac{M_{2\pi}}{a_0} \right)^{3/2} \frac{2}{n_{e_2}^2} \sum_{p=0}^{n_{e_2} - l_{e_2} - 1} (-1)^p \frac{[(n_{e_2} + l_{e_2})! (n_{e_2} - l_{e_2} - 1)!]^{1/2}}{(n_{e_2} - l_{e_2} - 1 - p)! p! (2l_{e_2} + 1 + p)!} \left(\frac{2Z\pi M}{n_{e_2} a_0} \right)^{l_{e_2} + p}$$

$$\cdot \left(\frac{M_{2\pi}}{a_0} \right)^{3/2} \frac{2}{n_{e_3}^2} \sum_{g=0}^{n_{e_3} - l_{e_3} - 1} (-1)^g \frac{[(n_{e_3} + l_{e_3})! (n_{e_3} - l_{e_3} - 1)!]^{1/2}}{(n_{e_3} - l_{e_3} - 1 - g)! g! (2l_{e_3} + 1 + g)!} \left(\frac{2Z\pi M}{n_{e_3} a_0} \right)^{l_{e_3} + g}$$

$$\cdot I(p, g, s) \quad (4.2)$$

and

$$I' = \frac{\Gamma(L_\pi + l + 1) \Gamma(l_e - l)}{A_\pi^{L_\pi + l + 1} A_c^{l_e - l}} \left(\frac{Ae^*}{Ae} \right)^{-(l_e + 1 - 2\eta)}$$

$$\cdot {}_2F_1(l_e + 1 - 2\eta, 2l_e + 2 - l_e + l; 2l_e + 2; \frac{-2ik}{Ae^*})$$

$$- \frac{\Psi A_\pi^{2l_e + 1 - l_e - L_\pi}}{|A_\pi + Ae|^{2l_e + 2}} \sum_{z=0}^{L_\pi + l_e - 2l_e - 2} \left(\frac{A_\pi}{A_\pi + Ae} \right)^z \Gamma(2l_e + 2 + z) \quad (4.3)$$

$$\cdot \left[\frac{\Gamma(L_\pi + l + 1)}{\Gamma(2l_e + 3 - l_e + l + z)} - \frac{\Gamma(L_\pi - l)}{\Gamma(2l_e + 2 - l_e - l + z)} \right] {}_2F_1(l_e + 1 - \eta, -z; 2l_e + 2; \frac{-2ik}{A_\pi + Ae^*})$$

when $(L_e - l) \geq (2l_{ef} + 2)$; and as

$$I'' = \frac{\Gamma(L_\pi + l + 1) \Gamma(2l_e + 2) \Gamma(2l_e + 1) \Gamma(-l_e - i\eta) (-1)^{l_e - l - 1} \chi(Ae^*)^{l_e}}{A_\pi^{L_\pi + l + 1} \Gamma(2l_e + 2 - l_e + l) \Gamma(l_e + 1 - i\eta) (2ik)^{2l_e + 1} A_c^{l_e - l - l_e - 1}}$$

$$\cdot {}_2F_1(1 - l_e + l, -l_e - i\eta; -2l_e; \frac{-2ik}{Ae^*})$$

$$- \frac{\Gamma(L_\pi + l + 1) \Psi \Gamma(2l_e + 2) \Gamma(l_e - i\eta) A_\pi^{2l_e + 1 - L_e + l}}{A_\pi^{L_\pi + l + 1} \Gamma(2l_e + 2 - l_e + l) \Gamma(l_e + 1 - 2\eta) (2ik) |A_\pi + Ae|^{2l_e}}$$

$$\cdot \sum_{d=0}^{l_e - l - 1} \frac{(1 + l - l_e)_d}{(1 - l_e + i\eta)_d} \left[\frac{|A_\pi + Ae|^2}{-2ik A_\pi} \right]^d \quad (4.4)$$

$$\cdot {}_2F_1(1 + d, -2l_e + d; l_e + 1 + 2\eta + d; \frac{Ae(A_\pi + Ae^*)}{2ik A_\pi})$$

$$- \frac{\Psi A_\pi^{2l_e + 1 - l_e - L_\pi}}{|A_\pi + Ae|^{2l_e + 2}} \sum_{z=0}^{L_\pi + l_e - 2l_e - 2} \left(\frac{A_\pi}{A_\pi + Ae} \right)^z \Gamma(2l_e + 2 + z)$$

$$\cdot \left[\frac{\Gamma(L_\pi + l + 1)}{\Gamma(2l_e + 3 - l_e + l + z)} - \frac{\Gamma(L_\pi - l)}{\Gamma(2l_e + 2 - l_e - l + z)} \right] {}_2F_1(l_e + 1 - 2\eta, -z; 2l_e + 2; \frac{-2ik}{A_\pi + Ae^*})$$

when $(2l_{ef} + 2) > (L_e - l)$.

Fortunately, this formula can be greatly simplified for the case in hand. First, only $l = |l_{\pi i} - l_{\pi f}|$ need be kept, as the higher terms are considerably smaller. Secondly, in helium, the ground state or $1s$ electron is the only one available to be ejected, hence $l_{ei} = 0$. The general formula then reduces to

$$\omega_{2 \rightarrow S} = \frac{Z^5 \pi}{\hbar} \left(\frac{e^2}{q_0} \right) \frac{1}{1 - e^{-2\pi\eta}} \frac{(2l_{\pi i} + 1)(2l_{\pi f} - 2l)!}{(2l + 1)!(2l_{\pi f} + 1)!} \binom{l_{\pi f}}{l}^2$$

$$\cdot \prod_{i=1}^l (i^2 B - i^2 + 1) \left(\frac{2Z e_i}{2Z\pi_2 M^2} \right)^l T(l)^2$$

$$T(l) = \langle r^l \rangle \left\{ \frac{\Gamma(2l+1) (l+1) \chi B^{l-1}}{\prod_{i=0}^l (i^2 B - i^2 + 1) 2^{2l}} + \frac{\Psi J(l)}{Q^l B} \right. \\ \left. + \frac{\Psi l D^2}{Q^{l+1}} + \frac{\Psi (2l)(l+2) D^3}{Q^{l+1} 3} \right\} \quad (4.5)$$

$$- \langle r^{l+2} \rangle \frac{\Psi}{Q^{l+1}} \left(\frac{Z e_i}{2Z\pi_2 M^2} \right) \frac{[1 + (2l+4)D]}{2(2l+3)}$$

$$+ \langle r^{l+3} \rangle \frac{\Psi}{Q^{l+1}} \left(\frac{Z e_i}{2Z\pi_2 M^2} \right)^{3/2} \frac{1}{3(2l+2)}$$

$$l = |l_2 - l_3|$$

$$D = M \left(\frac{Z e_i}{n_2} + \frac{Z}{n_3} \right)$$

$$l_{\pi f} = \max(l_2, l_3)$$

$$\chi = e^{-2\gamma \cot^{-1} \gamma}$$

$$1/\gamma^2 = \frac{4M}{n_3^2} - E_i$$

$$\Psi = e^{-2\gamma \cot^{-1} \gamma (1 + 1/\gamma)}$$

$$B = 1 + 1/\gamma^2$$

$$Q = (1 + 2D + BD^2)$$

$$\begin{aligned}
 \langle n^{\ell+N} \rangle &\equiv \left(\frac{Z}{n_i^2} \right) \left(\frac{Z}{n_s^2} \right) \left(\frac{n_i n_s}{n_2 + n_s} \right)^{\ell+N+3} \\
 &\cdot \left[(n_2 + \ell_i)! (n_2 - \ell_i - 1)! (n_s + \ell_s)! (n_s - \ell_s - 1)! \right]^{\frac{1}{2}} \\
 &\cdot \sum_{s=0}^{n_2 - \ell_i - 1} (-1)^s \binom{Z}{n_2 + n_s}^{\ell_i + s} \frac{1}{(n_2 - \ell_i - 1 - s)! s! (2\ell_i + 1 + s)!} \\
 &\cdot \sum_{z=0}^{n_s - \ell_s - 1} (-1)^z \binom{Z}{n_2 + n_s}^{\ell_s + z} \frac{1}{(n_s - \ell_s - 1 - z)! z! (2\ell_s + 1 + z)!} \\
 &\cdot (s + z + 2 + N + 2\ell_m)!
 \end{aligned}$$

The energies and effective Z_{ei} and $Z_{\pi i}$ for the higher $n_{\pi i}$ values have been taken from calculations done by Mausner (1975) and Russell (1970, B). For the calculations performed in this work, averages of the two values were taken. The values supplied by Mausner and Russell can be found in Appendix B.

$$|\langle n-1, n-2 | n^2 | n, n-2 \rangle|^2 = \frac{Z^{2\ell_i} (n-1)^{2\ell_i} n^{2\ell_i}}{(2n-1)^{2\ell_i}}$$

To obtain the Eisenberg and Kessler formula let

$$\psi^2 Q^{-2} \approx 1 \quad \text{and} \quad \frac{2\pi}{1-\alpha-2\pi} \approx \frac{1}{2}$$

This latter holds only when $\gamma \ll 1$.

4.2 Monopole Transition Rate Formula

The present work extends the formula given by Burbidge and de Borde to include all possible transitions. Furthermore it replaces the constant C_3 in their formula with an accurate but simple expression.

The monopole formula can be simply written as

$$\omega_{2 \rightarrow S} = \frac{1}{\hbar} \left(\frac{e^2}{a_0} \right) \frac{2^3 \pi}{3^2} \frac{1}{1 - e^{-2\gamma}} \frac{\Psi^2}{Q^2} \left(\frac{Z e_i}{2 Z \pi_i M^2} \right)^2 \cdot \left\{ \langle r^2 \rangle (1 + 4D) - \langle r^3 \rangle \left(\frac{Z e_i}{2 Z \pi_i M^2} \right)^{1/2} \right\}^2 \quad (4.6)$$

This formula is easily reduced to either the Burbidge and de Borde formula or the Eisenberg and Kessler one.

To obtain the Burbidge and de Borde formula merely replace $\Psi^2 Q^{-2}$ by C_3 and

$$\left\{ \langle r^2 \rangle (1 + 4D) - \langle r^3 \rangle \left(\frac{Z e_i}{2 Z \pi_i M^2} \right)^{1/2} \right\}^2$$

by

$$|\langle n-1, n-2 | r^2 | n, n-2 \rangle|^2 = \frac{2^{4k+3} (k-1)^{2k+5} n^{2k+4}}{(2k-1)^{4k+2}}$$

To obtain the Eisenberg and Kessler formula let

$$\Psi^2 Q^{-2} \approx 1 \quad \text{and} \quad \frac{2\pi}{1 - e^{-2\gamma}} \approx \frac{1}{\gamma}$$

This latter holds only when $\gamma \ll 1$.

For the lower energy transitions, $\gamma \approx 1$, the error introduced is substantial as

$$\frac{2\pi}{1 - e^{-2\pi}} = 6.28 \quad \text{while} \quad \frac{1}{\gamma} = 1$$

Even for $\gamma = \frac{1}{2}$,

$$\frac{2\pi}{1 - e^{-2\pi}} = 6.5 \quad \text{while} \quad \frac{1}{\gamma} = 2$$

The error introduced by allowing $\Psi^2 Q^{-2} = 1$ is not as great and has the opposite effect of the first error.

$$\frac{\langle r^2 \rangle}{\langle r^2 \rangle} = \frac{2 n_1^2 n_2^2}{(n_1^2 - n_2^2)} [6(n_1^2 + n_2^2) - 5l_1(n_1^2 - n_2^2)] \quad (4.8)$$

For $l_{if} > l_{fi}$ i.e. $\Delta l_{\gamma} = +1$

$$\omega_{if} = \frac{1}{\hbar} \left(\frac{e^2}{a_0} \right) \frac{2^5 \pi}{(1 - e^{-2\pi})} \frac{1}{3} \frac{f_0}{(2l_1 + 1)} \left(\frac{Z_0}{Z_0 M^2} \right) \frac{1}{B}$$

$$| \langle n \rangle |^2 \left[\chi - \frac{\Psi B}{10 Q^2} \left(\frac{Z_0}{Z_0 2 M^2} \right) \frac{\langle r^2 \rangle}{\langle r^2 \rangle} \right]^2 \quad (4.9)$$

where for $l_{if} > l_{fi}$

$$\frac{\langle r^2 \rangle}{\langle r^2 \rangle} = \frac{2 n_1^2 n_2^2}{(n_1^2 - n_2^2)} [6(n_1^2 + n_2^2) + 5(l_1 + 1)(n_1^2 - n_2^2)] \quad (4.10)$$

In general, for dipole transitions

4.3 Dipole Transition Rate Formulae

The dipole transition formula offered here is similar to the Burbidge and de Borde formula but is applicable to all possible transitions and, unlike the Eisenberg and Kessler formula, contains the penetration terms.

For $l_{\pi i} > l_{\pi f}$ i.e. $\Delta l_{\pi} = -1$

$$\omega_{2 \rightarrow 5} = \frac{1}{\hbar} \left(\frac{e^2}{a_0} \right) \frac{2^5 \pi}{(1 - e^{-2\pi\delta})} \frac{1}{3} \frac{l_{\pi i}}{(2l_{\pi i} + 1)} \left(\frac{Z_{e_j}}{Z_{\pi_i} M^2} \right) \frac{1}{B} \cdot |\langle n \rangle|^2 \left\{ \chi - \frac{\Psi B}{10 Q^2} \left(\frac{Z_{e_j}}{2 Z_{\pi_i} M^2} \right) \frac{\langle r^3 \rangle}{\langle r' \rangle} \right\}^2 \quad (4.7)$$

where for $l_{\pi i} > l_{\pi f}$

$$\frac{\langle r^3 \rangle}{\langle r' \rangle} = \frac{2 n_i^2 n_f^2}{(n_i^2 - n_f^2)} \left[6(n_i^2 + n_f^2) - 5l_i(n_i^2 - n_f^2) \right] \quad (4.8)$$

For $l_{\pi f} > l_{\pi i}$ i.e. $\Delta l_{\pi} = +1$

$$\omega_{2 \rightarrow 5} = \frac{1}{\hbar} \left(\frac{e^2}{a_0} \right) \frac{2^5 \pi}{(1 - e^{-2\pi\delta})} \frac{1}{3} \frac{l_{\pi f}}{(2l_{\pi f} + 1)} \left(\frac{Z_{e_j}}{Z_{\pi_i} M^2} \right) \frac{1}{B} \cdot |\langle n \rangle|^2 \left\{ \chi - \frac{\Psi B}{10 Q^2} \left(\frac{Z_{e_j}}{Z_{\pi_i} 2 M^2} \right) \frac{\langle r^3 \rangle}{\langle r' \rangle} \right\}^2 \quad (4.9)$$

where for $l_{\pi f} > l_{\pi i}$

$$\frac{\langle r^3 \rangle}{\langle r' \rangle} = \frac{2 n_i^2 n_f^2}{(n_i^2 - n_f^2)} \left[6(n_i^2 + n_f^2) + 5(l_f + 1)(n_i^2 - n_f^2) \right] \quad (4.10)$$

In general, for dipole transitions

$$\omega_{2 \rightarrow S} = \frac{1}{\hbar} \left(\frac{e^2}{q_0} \right) \frac{Z^5 \pi}{(1 - e^{-2\pi\gamma})} \frac{1}{3} \frac{\max(l_i, l_f)}{(2l_{n_2} + 1)} \frac{1}{B}$$

$$| \langle n \rangle |^2 \left\{ \chi - \frac{\Psi B}{10 Q^2} \left(\frac{Z e_i}{2 Z \pi_i M^2} \right) \right. \quad (4.11)$$

5.1. The Total Transition Rate

$$\cdot \frac{2 n_i^2 n_f^2}{(n_i^2 - n_f^2)} \left[6(n_i^2 + n_f^2) + 5 \operatorname{sgn}(\Delta l_r) \max(l_i, l_f) (n_i^2 - n_f^2) \right] \left. \right\}^2$$

By employing the same approximations as before, these formulae can easily be reduced to either the Burbidge and de Borde formula or the Eisenberg and Kessler one.

Tables III and IV, which follow immediately, highlight the main features of these results.

Table III gives the total transition rate from a given state to all states such that $|l_i - l_f| \leq 3$ and where n_f ranges over the three highest allowed values. For $n_i = 2$ through 12, transitions to the next lower state are allowed, i.e. $n_f = n_i - 1$, and for these initial states, $\omega_T(n_i, l_i)$ increases with n_i . For $n_i = 13$ and 14 however, transitions must be to the $n_f = 11$ and 12 states respectively and for $n_i = 15, 16$ and 17, $n_f = 12, 13,$ and 14. Because of this the transition rates from these states are considerably reduced.

Also the transitions from the $l_i = 15$ and 16 states are repressed as the pion must undergo a quadrupole or octopole transition in order to reach the first allowed state.

CHAPTER 5

THE PRESENT WORK. NUMERICAL RESULTS

5.1. The Total Transition Rate

The Auger transition rates (in pionic helium) for transitions from all states having initial principal quantum number, n_i , equal to 2 through 12, 14 and 17 have been calculated.

Tables III and IV, which follow immediately, highlight the main features of these results.

Table III gives the total transition rate from a given state to all states such that $|\ell_i - \ell_f| \leq 3$ and where n_f ranges over the three highest allowed values. For $n_i = 2$ through 12, transitions to the next lower state are allowed, i.e. $n_f = n_i - 1$, and for these initial states, $\omega_T(n_i, \ell_i)$ increases with n_i . For $n_i = 13$ and 14 however, transitions must be to the $n_f = 11$ and 12 states respectively and for $n_i = 15, 16$ and 17, $n_f = 12, 13$, and 14. Because of this the transition rates from these states are considerably reduced.

Also the transitions from the $\ell_i = 15$ and 16 states are repressed as the pion must undergo a quadrupole or octopole transition in order to reach the first allowed state.

Generally the majority of transitions are dipole transitions to the highest allowed orbit. Denoting the sum of these two transitions as ω_0 , Table IV charts several values of ω_0/ω_T . It is most evident that this is not a good approximation, especially for the higher $n_{\pi i}$ orbits where the Auger Effect is most likely to occur.

$\omega_T = [\text{entry}] \times 10^{23}$

$n_{\pi i}$	0	3	6	9	12	15	16
17	.776	.886	1.12	1.23	.860	.137	.047
14	.607	.736	1.01	1.17	.630		
11	3.31	4.61	8.63	14.8			
8	1.17	1.86	3.87				
5	.081	.276					

TABLE III

TABLE IV

The Total Auger Transition Rate, ω_T , as a Function of $n_{\pi i}$ and $l_{\pi i}$.

$\omega_T = [\text{entry}] \times 10^{14}$

$l_{\pi i}$	0	3	6	9	12	15	16
17	.776	.886	1.12	1.23	.860	.137	.047
14	.607	.736	1.01	1.17	.630		
11	3.31	4.61	8.63	14.8	.63	.00	
8	1.17	1.86	3.87	.72	.86		
5	.081	.276	.65	.84			

5.2 Monopole Transition Rates

Table V shows the percentage contribution of the monopole rates to the total rate. From these it can be seen that monopole transitions are dominant when the initial value of n is high, but initial l is low. For example, when $(n_i, l_i) = (17, 3)$ the contribution of the monopole rates to the total rate is 59%. Even when the initial value of n is low, monopole transitions still contribute a considerable portion of the total rate - 30% for $(n_i, l_i) = (5, 0)$.

TABLE IV

ω_0/ω_T , where ω_0 is the Sum of the Two Dipole Transitions into the Highest Allowed Orbit as a Function of $n_{\pi i}$ and $l_{\pi i}$.

$l_{\pi i}$	0	3	6	9	12	15	16
17	.16	.22	.33	.47	.63	.00	-
14	.37	.44	.56	.72	.86		
11	.49	.56	.65	.84			
8	.41	.60	.85				
5	.64	.92					

5.2 Monopole Transition Rates

Table V shows the percentage contribution of the monopole rates to the total rate. From these it can be seen that monopole transitions are dominant when the initial value of n is high, but initial l is low. For example, when $(n_i, l_i) = (17, 3)$ the contribution of the monopole rates to the total rate is 59%. Even when the initial value of n is low, monopole transitions still contribute a considerable portion of the total rate - 30% for $(n_i, l_i) = (5, 0)$.

The mistaken concept that monopole transitions are not significant is due to the original calculation done by Burbidge and de Borde. They considered only monopole transitions into circular orbits, which when compared to the dipole transition into the same orbit are indeed inconsequential (see Table VI).

The Eisenberg and Kessler formula did not contain this restriction; and, in fact, when viewing their version of a muon cascade in carbon, the high degree of stability in the population of the high n_i , low l_i states indicates a high monopole rate between these states.

TABLE VI
 MONOPOLE TRANSITIONS INTO CIRCULAR ORBITS AS COMPARED
 TO DIPOLE TRANSITIONS INTO THE SAME ORBIT

TABLE V

Contribution of the Monopole Transitions $[\omega_{\Delta\ell=0}]$ to the
 Total Transition Rate $[\omega_T]$ as a Function of $n_{\pi i}$ and $\ell_{\pi i}$.

$n_{\pi i}$	$\ell_{\pi i}$	0	3	6	9	12	15
17	(3,2)	.68	.59	.43	.27	.11	-
14	(3,2)	.47	.37	.22	.10	-	-
11	(3,2)	.29	.24	.15	.05	-	-
8	(4,3)	.47	.27	.06	-	-	-
5	(4,3)	.30	.04	-	-	-	-

TABLE VI

MONOPOLE TRANSITIONS INTO CIRCULAR ORBITS AS COMPARED
TO DIPOLE TRANSITIONS INTO THE SAME ORBIT

TRANSITION	TRANSITION RATE	ω_M/ω_D
(2,1)→(1,0)	.49817 x 10 ¹¹	.0179
(2,0)→(1,0)	.89392 x 10 ⁹	
(3,2)→(2,1)	.16280 x 10 ¹³	.0187
(3,1)→(2,1)	.30488 x 10 ¹¹	
(4,3)→(3,2)	.11560 x 10 ¹⁴	.0223
(4,2)→(3,2)	.25755 x 10 ¹²	
(5,4)→(4,3)	.43896 x 10 ¹⁴	.0274
(5,3)→(4,3)	.12026 x 10 ¹³	
(6,5)→(5,4)	.11777 x 10 ¹⁵	.0337
(6,4)→(5,4)	.39709 x 10 ¹³	

*By a statistical distribution, it is meant that a state with angular momentum eigenvalue l , will have $2l + 1$ states, one for each azimuthal eigenvalue m .

5.3 Dipole Transition Rates

Tables VII and VIII show the relative percentages of the two dipole rates. The dipole transitions where the pion loses one unit of angular momentum ($\Delta\ell_{\pi} = -1$) are much more probable than those where the pion gains one unit, the latter being significant only when the initial ℓ value is zero ($\ell_{\pi i} = 0$). The dipole transitions are usually dominant, especially for low initial n values, and, of course, for transitions between circular orbits.

The combined prominence of the monopole and dipole ($\Delta\ell_{\pi} = -1$) rates tend to keep the pions away from the circular orbits (see Figure 3). However once a pion enters a circular orbit, it will cascade to the lower states through the other circular orbits. In particular if the pions are initially distributed statistically¹ in the $n_{\pi i} = 17$ state, then 32% of all pions are initially in the $\ell_{\pi i} = 14, 15$ and 16 states. 75% of these pions will descend to the $(n_f, \ell_f) = (14, 13)$ state after the first transition, thereby placing 25% of all pions into a circular orbit early in the cascade.

¹By a statistical distribution, it is meant that a state with angular momentum eigenvalue ℓ , will have $2\ell + 1$ states, one for each azimuthal eigenvalue m .

TABLE VII

Contribution of the Dipole [$\Delta\ell_{\pi} = -1$] Transition Rate [$\omega_{\Delta\ell = -1}$] to the Total Transition Rate [ω_T] as a Function of $n_{\pi i}$ and $\ell_{\pi i}$.

$\ell_{\pi i}$	0	3	6	9	12
$n_{\pi i}$					
17	.28	.35	.56	.72	.78
14	.50	.54	.76	.88	.86
11	.55	.60	.75	.88	
8	.66	.65	.89		
5	.67	.93			

EXAMPLES OF BRANCHING RATIOS OF AUGER TRANSITIONS
INDICATING THE TENDENCY AWAY FROM THE CIRCULAR ORBITS

TABLE VIII

Contribution of the Dipole [$\Delta\ell = +1$] Transition Rate
[$\omega_{\Delta\ell=+1}$] to the Total Transition Rate [ω_T] as a Function of
 $n_{\pi i}$ and $\ell_{\pi i}$.

$n_{\pi i}$ \ $\ell_{\pi i}$	0	3	6	9	12
17	.28	.04	.01	.00	.00
14	.50	.08	.01	.00	-
11	.55	.06	.00	-	-
8	.46	.03	-	-	-
5	.67	-	-	-	-

FIGURE 3

EXAMPLES OF BRANCHING RATIOS OF AUGER TRANSITIONS
INDICATING THE TENDENCY AWAY FROM THE CIRCULAR ORBITS

Generally higher multipole transitions are not con-

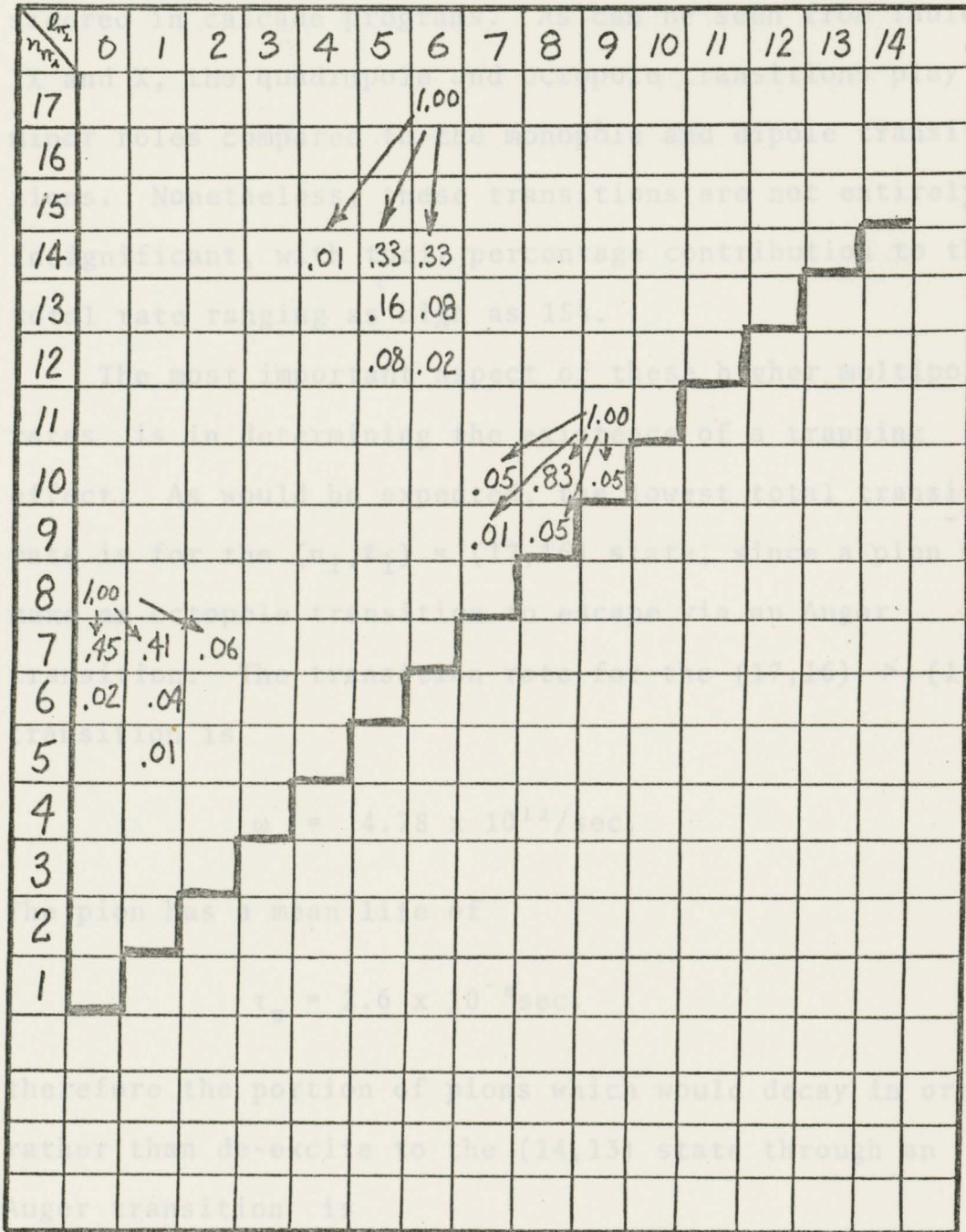


FIGURE 3

5.4 Higher Multipole Rates at, as long as there is an electron in the atom, there is no trapping effect.

Generally higher multipole transitions are not considered in cascade programs. As can be seen from Tables IX and X, the quadrupole and octopole transitions play minor roles compared to the monopole and dipole transitions. Nonetheless, these transitions are not entirely insignificant, with their percentage contribution to the total rate ranging as high as 15%.

The most important aspect of these higher multipole rates is in determining the existence of a trapping effect. As would be expected, the lowest total transition rate is for the $(n_i, l_i) = (17, 16)$ state, since a pion must make an octopole transition to escape via an Auger transition. The transition rate for the $(17, 16) \rightarrow (14, 13)$ transition is

$$\omega = 4.78 \times 10^{12}/\text{sec.}$$

The pion has a mean life of

$$\tau_{\pi} = 2.6 \times 10^{-8} \text{sec.}$$

therefore the portion of pions which would decay in orbit rather than de-excite to the $(14, 13)$ state through an Auger transition is

$$\frac{1}{1 + \tau_{\pi} \omega} \sim 10^{-5}$$

It can then be concluded that, as long as there is an electron in the atom, there is no trapping effect.

If both electrons have already been ejected, then external effects, such as the External Auger or the Stark Effect, would have to be considered in determining whether or not the trapping effect exists.

Contribution of the Quadrupole [$\Delta l = + 2$] Transition Rate [$\omega_{Q\Delta l}$] to the Total Transition Rate [ω_T] as a Function of n_{r1} and l_{r1} .

l_{r1}	0	3	6	9	12	15
17	.03	.01	.01	.00	.10	.91
14	.02	.01	.01	.00	.13	
11	.15	.09	.08	.06		
8	.07	.05	.04			
5	.03	.03				

TABLE IX

Contribution of the Quadrupole [$\Delta\ell = + 2$] Transition Rate [$\omega_{\Delta\ell}$] to the Total Transition Rate [ω_T] as a Function of $n_{\pi i}$ and $\ell_{\pi i}$.

$\ell_{\pi i}$	0	3	6	9	12	15
17	.03	.01	.01	.00	.10	.91
14	.02	.01	.01	.00	.13	.09
11	.15	.09	.08	.06	.01	
8	.07	.05	.04	.00		
5	.03	.03	.00			

5.5 The Dipole, Quadrupole and Octopole Transition Rates as a Function of $n_{\pi i}$ and $l_{\pi i}$

Tables XI, XII, and XIII chart the transition rates for several transitions where $\Delta n_{\pi} = \Delta l_{\pi}$ are equal to

TABLE X

-1, -2, and -3 respectively. The transition rates of

all three types of transitions, dipole quadrupole and

Contribution of the Octopole [$\Delta l_{\pi} = \pm 3$] Transition Rate

[$\omega_{\Delta l}$] to the Total Transition Rate [ω_T] as a Function of

$n_{\pi i}$ and $l_{\pi i}$.

the quadrupole and octopole transitions the rates for a particular value of $l_{\pi i}$ tend to remain (roughly) constant as $n_{\pi i}$ increases.

The general increase as $l_{\pi i}$ increases is unmistakable

$l_{\pi i}$	0	3	6	9	12	15
17	.00	.00	.00	.00	.01	.09
14	.00	.00	.00	.00	.01	
11	.01	.01	.00	.00		
8	.00	.00	.00			
5	.00					

roughly equivalent for low values of $l_{\pi i}$, but diverge as $l_{\pi i}$ increases. A similar relation is often true for the two octopole or two quadrupole transition rates.

5.5 The Dipole, Quadrupole and Octopole Transition Rates as a Function of $n_{\pi i}$ and $l_{\pi i}$

Tables XI, XII, and XIII chart the transition rates for several transitions where $\Delta n_{\pi} = \Delta l_{\pi}$ are equal to -1, -2, and -3 respectively. The transition rates of all three types of transitions, dipole quadrupole and octopole, show a definite increase with $l_{\pi i}$. Only for the dipole transitions, however, do the rates increase with $n_{\pi i}$. For the quadrupole and octopole transitions the rates for a particular value of l_i tend to remain (roughly) constant as n_i increases.

The general increase as l_i increases is unmistakable and J. E. Russell's values for the (17,16) \rightarrow (14,13) and the (16,15) \rightarrow (13,12) transition rates, $9 \times 10^8/\text{sec.}$ and $6 \times 10^9/\text{sec.}$ respectively, are completely inconsistent with these results.

Figures 4, 5, 6 and 7 show the general dependence of the transition rate on multipolarity. It is interesting to note that the monopole rate and both dipole rates are roughly equivalent for low values of l_i , but diverge as l_i increases. A similar relation is often true for the two octopole or two quadrupole transition rates.

TABLE XI

TABLE XII

The Transition Rate for $\Delta n_{\pi} = \Delta \ell_{\pi} = -1$ Transitions as a
Function of $n_{\pi i}$ and $\ell_{\pi i}$.

$\ell_{\pi i}$ \ $n_{\pi i}$	1	4	7	10
11	$.01^{15}$	$.32^{15}$	$.72^{15}$	$.16^{16}$
9	$.55^{14}$	$.21^{15}$	$.55^{15}$	
7	$.25^{14}$	$.11^{15}$		
5	$.66^{13}$			

A^B means $A \times 10^B$

A^B means $A \times 10^B$

TABLE XII

The Transition Rate for $\Delta n_{\pi} = \Delta l_{\pi} = \pm 2$ Transitions as a Function of $n_{\pi i}$ and $l_{\pi i}$.

$l_{\pi i}$	2	5	8	11	13
14	$.56^{12}$	$.96^{12}$	$.26^{12}$	$.18^{13}$	$.16^{14}$
11	$.16^{13}$	$.99^{11}$	$.89^{12}$		
8	$.27^{12}$	$.14^{11}$			
5	$.76^{10}$				

A^B means $A \times 10^B$

TABLE XIII

The Transition Rate for $\Delta n_{\pi} = \Delta l_{\pi} = -3$ Transitions as a Function of $n_{\pi i}$ and $l_{\pi i}$.

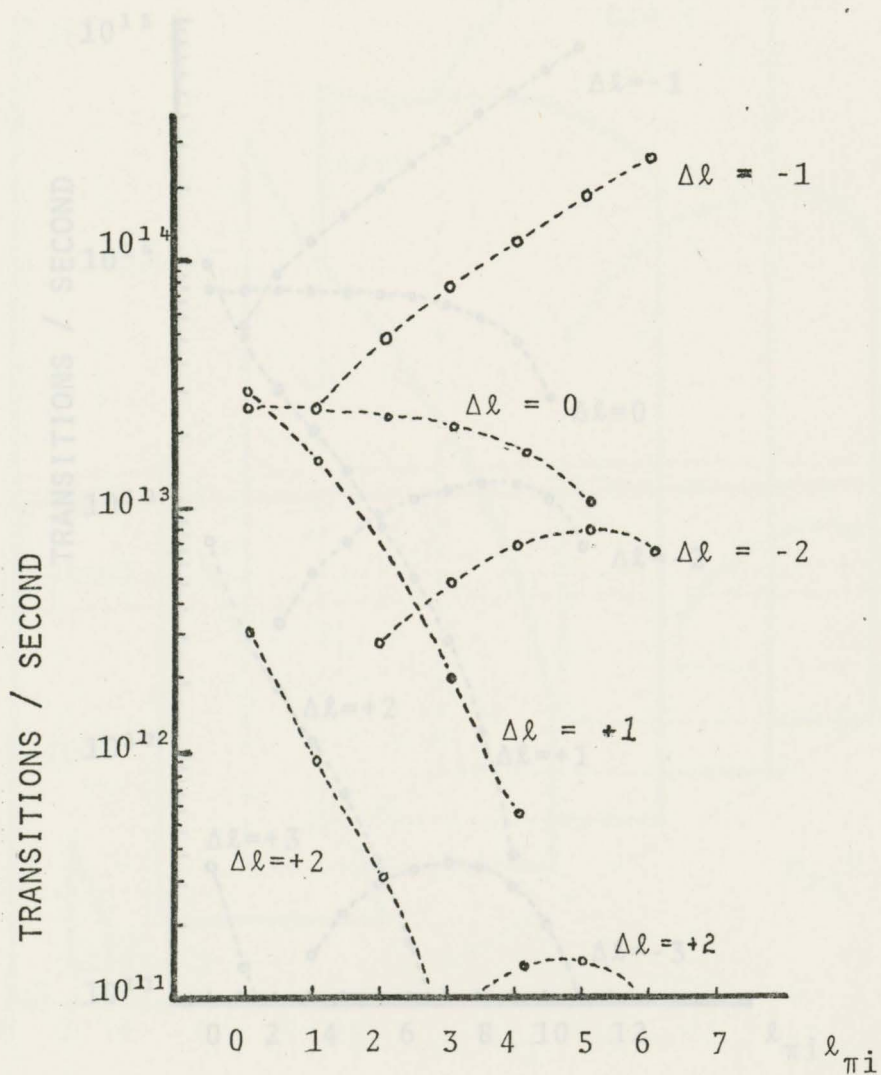
$l_{\pi i}$	3	6	9	13	16
$n_{\pi i}$					
17	.22 ¹⁰	.32 ¹¹	.39 ¹²	.57 ¹²	.48 ¹³
14	.48 ⁸	.45 ¹⁰	.33 ¹¹	.16 ¹²	
11	.23 ⁸	.66 ¹¹	.15 ¹¹		
8	.15 ⁹	.62 ¹⁰			
5	.29 ⁸				

A^B means $A \times 10^B$

DEPENDENCE OF THE TRANSITION RATE ON MULTIPOLARITY FOR

$n_{\pi i} = 7$

FIGURE 4



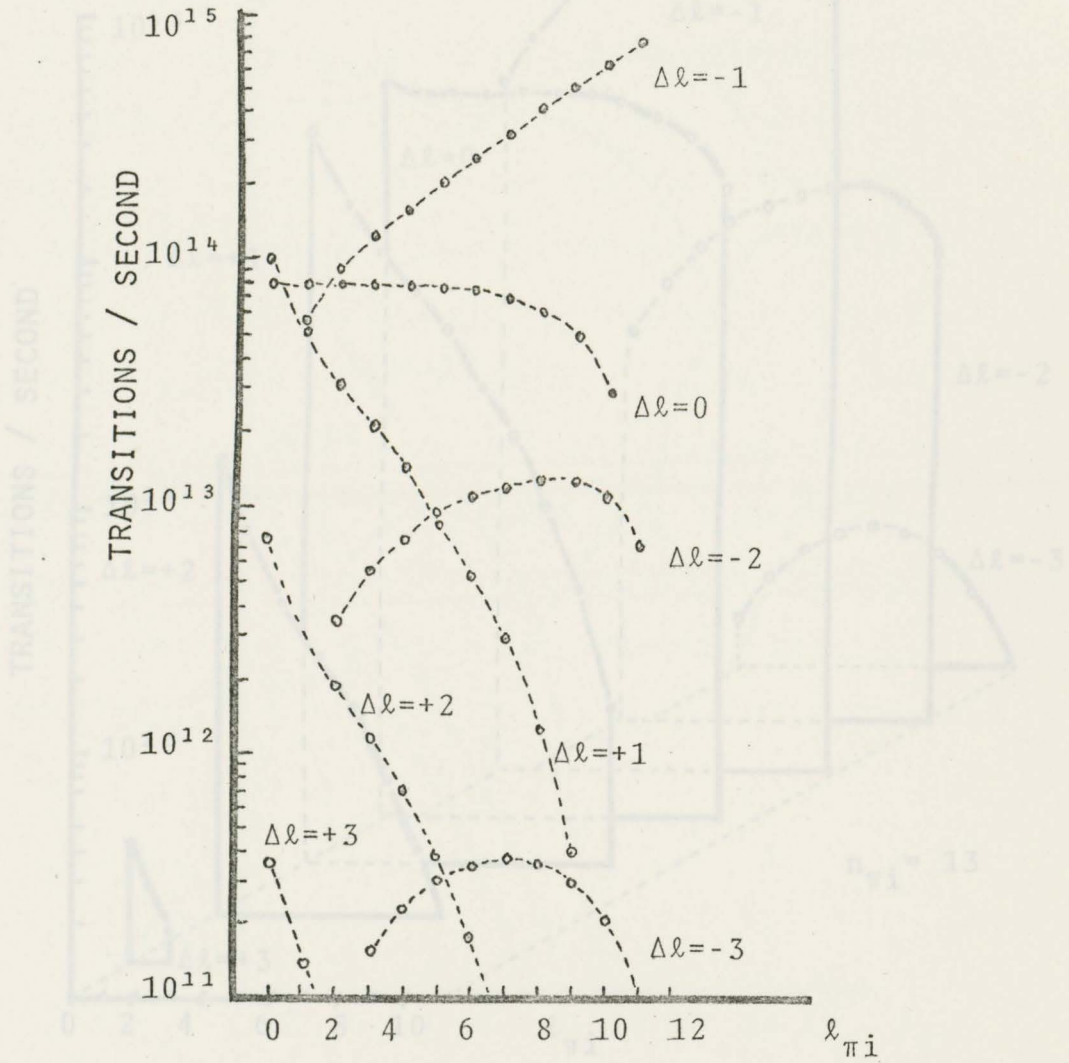
DEPENDENCE OF THE TRANSITION RATE ON MULTIPOLARITY FOR

DEPENDENCE OF THE TRANSITION RATE ON MULTIPOLARITY FOR

$$n_{\pi i} = 7$$

FIGURE 5

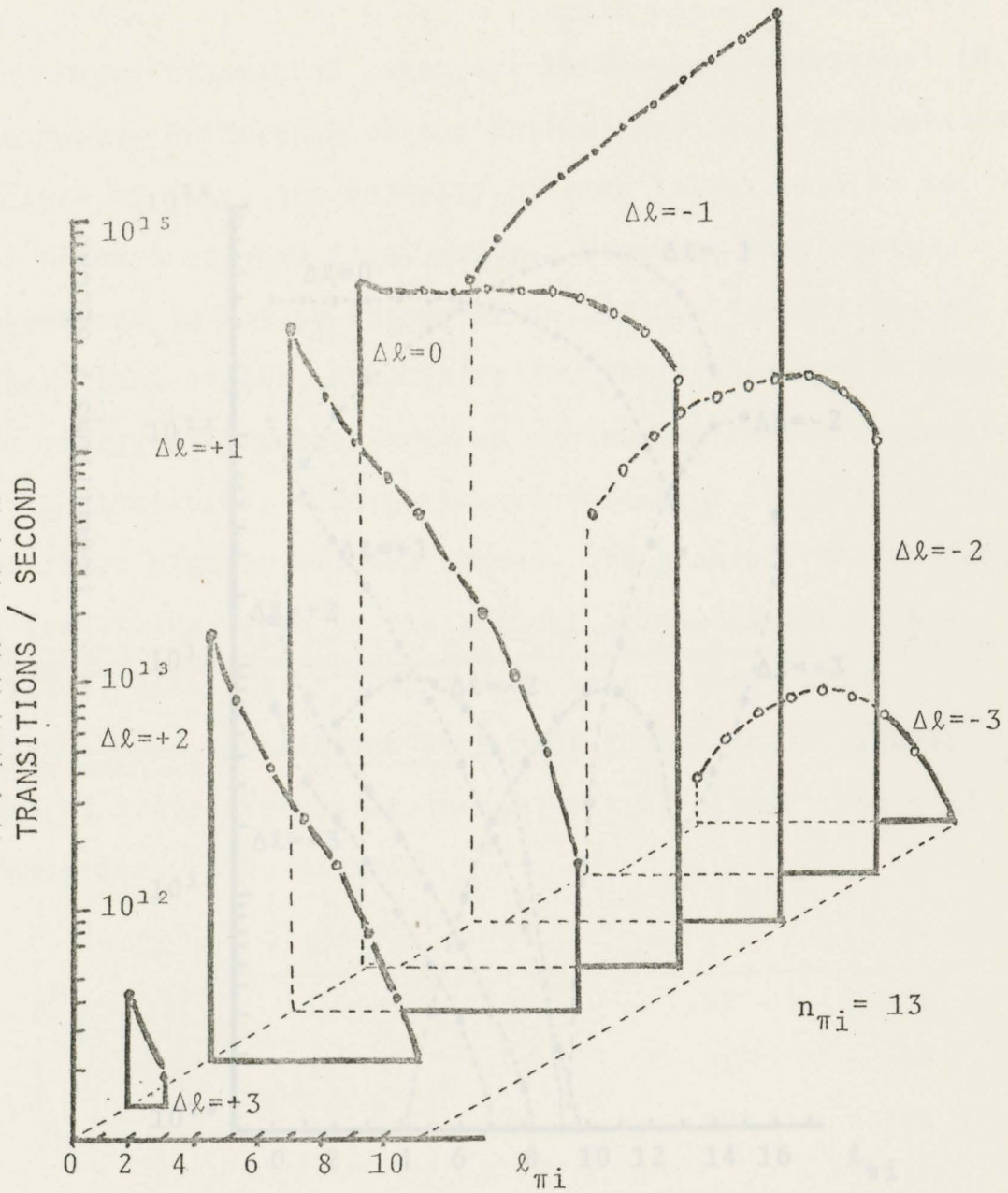
FIGURE 4



DEPENDENCE OF THE TRANSITION RATE ON MULTIPOLARITY FOR

$$n_{\pi i} = 13$$

FIGURE 5



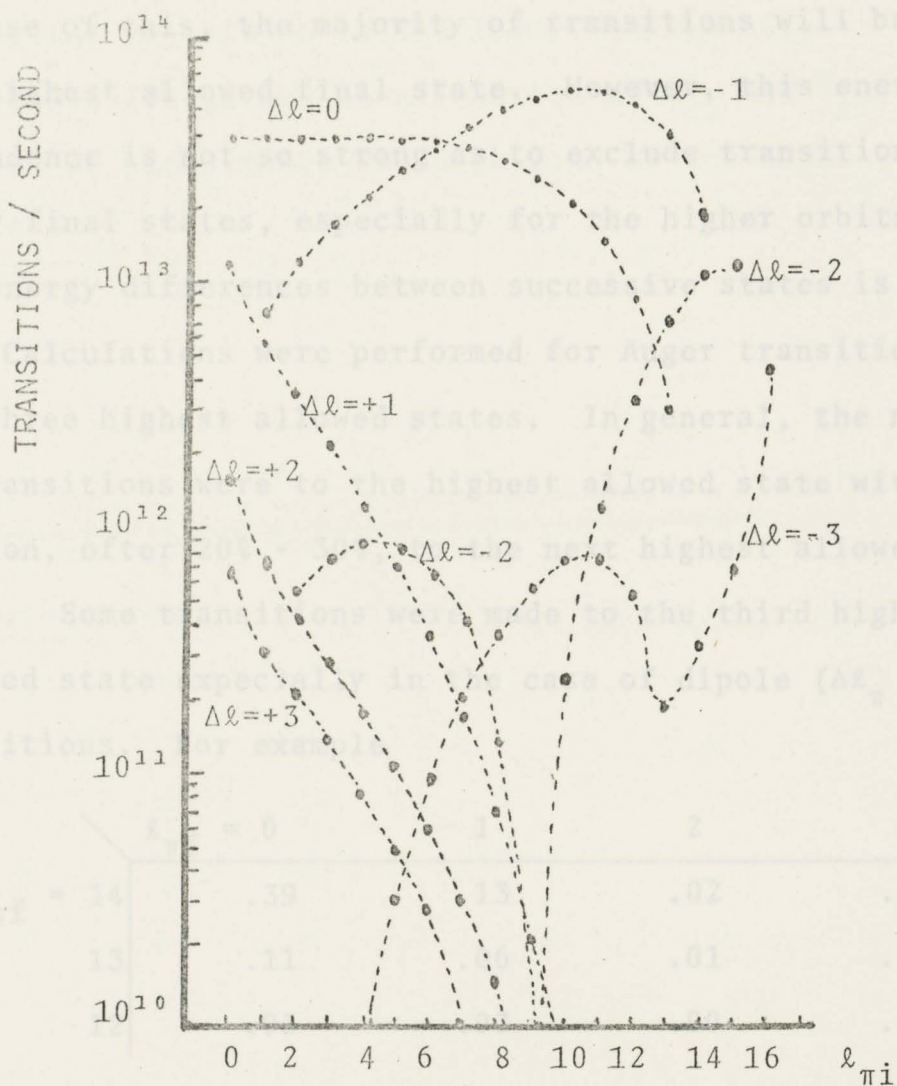
DEPENDENCE OF THE TRANSITION RATE ON MULTIPOLARITY FOR EXPANDED VIEW OF THE CASE DISPLAYED IN FIGURE 5.

FIGURE 6

5.6 Transition Rates as a Function of $(n_{\pi i} - n_{\pi f})$

Auger transition rates are inversely proportional to the energy difference of the initial and final pion states.

Because of this, the majority of transitions will be to the lowest energy final state. This energy dependence is of course not exclusive to Auger transitions to other final states, especially for the higher orbits when the energy differences between successive states is small. Calculations were performed for Auger transitions to the five highest allowed states. In general, the majority of transitions to the highest allowed state with a portion, often the majority, of high energy allowed state. Some transitions will be to the third highest allowed state in the case of dipole ($\Delta\ell = -1$) transitions.



DEPENDENCE OF THE TRANSITION RATE ON MULTIPOLARITY FOR

$$n_{\pi i} = 17$$

Figure 8

Branching Ratios

For Auger Transitions $n_{\pi i} = 17, l_{\pi i} = 0$ State

FIGURE 7

5.6 Transition Rates as a Function of $(n_{\pi i} - n_{\pi f})$

transitions. For the lower $n_{\pi i}$ states almost all transitions Auger transition rates are inversely proportional to the energy difference of the initial and final pion states. Because of this, the majority of transitions will be to the highest allowed final state. However, this energy dependence is not so strong as to exclude transitions to other final states, especially for the higher orbits when the energy differences between successive states is small.

Calculations were performed for Auger transitions to the three highest allowed states. In general, the majority of transitions were to the highest allowed state with a portion, after 20% - 30%, to the next highest allowed state. Some transitions were made to the third highest allowed state especially in the case of dipole ($\Delta l_{\pi} = -1$) transitions. For example

	$l_{\pi f} = 0$	1	2	3
$n_{\pi f} = 14$.39	.13	.02	.00
13	.11	.06	.01	.00
12	.03	.03	.00	.00

Figure 8

Branching Ratios

For Auger Transitions From the $n_{\pi i} = 17, l_{\pi i} = 0$ State

A general pattern emerged from the rates for all transitions. For the lower $n_{\pi i}$ states almost all transitions (90% - 100%) were made to the highest allowed state. However, as $n_{\pi i}$ increased so did the portion of pions making the transition to the lower final orbits.

Table XIV gives, as a function of $n_{\pi i}$ and $\ell_{\pi i}$, the portion of pions which would descend to the highest possible state.

$\ell_{\pi i}$	0	3	6	9	12	15
17	.69	.68	.67	.69	.79	.94
14	.78	.77	.76	.81	.90	
11	.83	.83	.86	.94		
8	.92	.91	.95			
5	.97	1.00				

The Role of the Penetration Terms for Dipole Transition Rates

TABLE XIV

The Contribution to the Total Transition Rate from the Transitions into the Highest Allowed Orbit.

$\ell_{\pi i}$	0	3	6	9	12	15
17	.69	.68	.67	.69	.79	.94
14	.78	.77	.76	.81	.96	
11	.83	.83	.86	.94		
8	.92	.91	.95			
5	.97	1.00				

$$\frac{\omega_{\Delta n=\min}}{\omega_T}$$

$$\omega_T$$

In 1974, Raff, Viellier, and Alder (Alder, 1974) did a calculation of the penetration factor for muonic thallium. Even though their calculations were more sophisticated, taking current-current and retardation effects into consideration in their matrix elements (i.e.

5.7 The Role of the Penetration Terms for Dipole Transition Rates

So far, only approximate Auger transition rates, evaluated in the "no penetration" approximation have been used to calculate x-ray intensity ratios in the pionic (or muonic) cascade. However, even when $r_e > r_\pi$, the pion and electron charge densities are still strongly overlapping in the region between the nucleus and the K-shell electron. Because of this, penetration effects have been found to be rather important.

In figure 9, the penetration factor $P = (\omega/\omega_N) - 1$, where ω_N is the transition rate calculated without the penetration terms, is investigated for dipole transitions. The factor P has been graphed for three values of $n_{\pi i}$ as a function of ℓ_i ; only $\Delta\ell_\pi = -1$ has been considered.

The significance of penetrations effects is immediately seen from the magnitude of P . The sign of P (i.e. $P < 0$) indicates that inclusion of the penetration terms depresses the transition rate. Also the magnitude of P increases with $\ell_{\pi i}$ but decreases with $n_{\pi i}$; a reflection, no doubt, of the relation $\langle r \rangle \sim 3n^2 - \ell(\ell + 1)$.

In 1974, Raff, Viollier, and Alder (Alder, 1974) did a calculation of the penetration factor for muonic thallium. Even though their calculations were more sophisticated, taking current-current and retardation effects into consideration in their matrix elements (i.e.

a relativistic approach) the general dependence of the penetration factor P on $n_{\pi i}$ and $l_{\pi i}$ is strikingly similar.

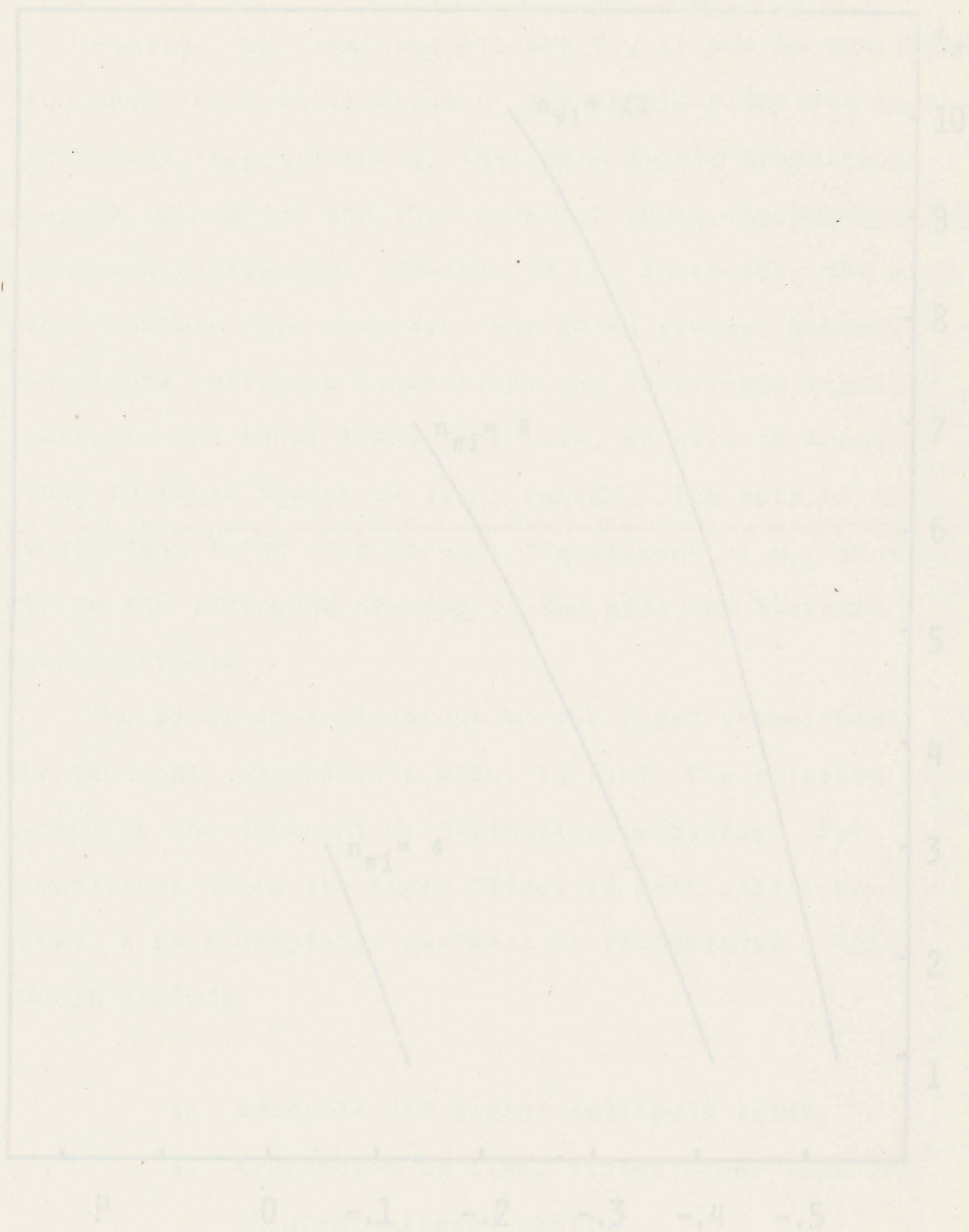


FIGURE 9

THE PENETRATION FACTOR $P = \omega/\omega_n - 1$ AS A FUNCTION OF $n_{\pi i}$ AND $l_{\pi i}$ FOR DIPOLE TRANSITIONS

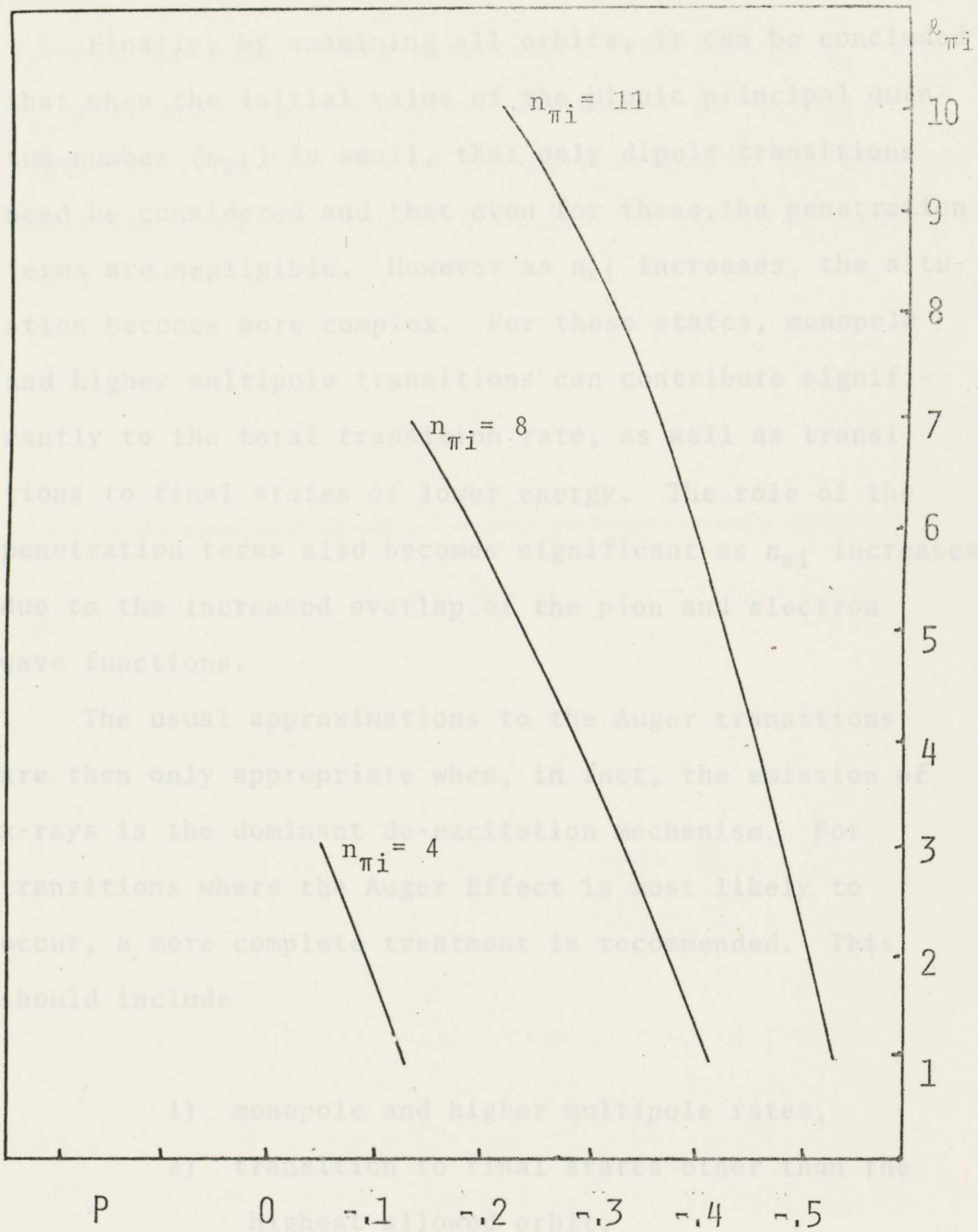


FIGURE 9

5.8 Conclusions and Recommendation with Regard to the Calculation of the Internal Mesic Auger Rates

Finally, by examining all orbits, it can be concluded that when the initial value of the pionic principal quantum number ($n_{\pi i}$) is small, that only dipole transitions need be considered and that even for these, the penetration terms are negligible. However as $n_{\pi i}$ increases, the situation becomes more complex. For these states, monopole and higher multipole transitions can contribute significantly to the total transition rate, as well as transitions to final states of lower energy. The role of the penetration terms also becomes significant as $n_{\pi i}$ increases due to the increased overlap of the pion and electron wave functions.

The usual approximations to the Auger transitions are then only appropriate when, in fact, the emission of x-rays is the dominant de-excitation mechanism. For transitions where the Auger Effect is most likely to occur, a more complete treatment is recommended. This should include

- 1) monopole and higher multipole rates,
- 2) transition to final states other than the highest allowed orbit,
- 3) penetration terms.

Although numerical calculations have been carried out only for helium, the results are applicable to all mesic atoms. This follows directly from the form of the general formula for Auger transition rates. The factors Z_e and Z_π never appear by themselves but always as (Z_e/Z_π) , a slowly varying function of the nuclear charge Z . No great deviation from the results obtained for helium is expected for the other elements.

Abramowitz, M. and Stegun, I. 1978. Handbook of Mathematical Functions. Dover Publications, Inc., New York.

Akylas, V.R. and Vogel, P. 1977. Improvements on the cascade of negative muons in atoms. In abstract volume of the 7th International Conference on High-Energy Physics and Nuclear Structure, p. 277, CERN-Swiss Institute for Nuclear Research, Switzerland.

Akylas, V.R. and P. Vogel, P.K. Haff, A. Winther. 1978. Muon capture in atoms, crystals and molecules. Nucl. Phys., 254A, 445.

Alder, K and U. Raff, R.D. Viollier. 1974. Penetration effects in converted muonic transitions. Nucl. Phys., 223A, 429.

Anderhub, H., H. Hofer, E. Kottmann, P. LeCoultré, D. Makowiecki, O. Pittoria, B. Sapp, P.G. Seiler, N. Niklitch, D. Tazou, P. Truttmann, A. Zehnder and Ch. Tschaligr. 1977. Search for the metastable $2s$ state in muonic hydrogen. Phys. Lett., 71B, 443.

REFERENCES

- Abela, R., G. Backenstoss, A. Brandao D'Oliveira, M. Izycki, H.O. Meyer, I. Schwanner, L. Tauscher, P. Blum, W. Fetscher, D. Gotta, H. Koch, H. Poth, L.M. Simons. 1977. Pionic x-ray transitions in ^3He . *Phys.Lett.*, 68B, 429.
- Abramowitz, M. and Stegun, I. 1970. Handbook of Mathematical Functions. Dover Publications, Inc., New York.
- Akylas, V.R. and Vogel, P. 1977. Improvements on the cascade of negative muons in atoms. In abstract volume of the 7th International Conference on High-Energy Physics and Nuclear Structure, p 277, Sin-Swiss Institute for Nuclear Research, Switzerland.
- Akylas, V.R. and P. Vogel, P.K. Haff, A. Winther. 1975. Muon capture in atoms, crystals and molecules. *Nucl. Phys.*, 254A, 445.
- Alder, K. and U. Raff, R.D. Viollier. 1974. Penetration effects in converted muonic transitions. *Nucl.Phys.*, 223A, 429.
- Anderhub, H., H. Hofer, F. Kottmann, P. LeCoultré, D. Makowieski, O. Pitzurra, B. Sapp, P.G. Seiler, M. Wählchli, D. Taquq, P. Truttmann, A. Zehnder and Ch. Tschalär. 1977. Search for the metastable 2s state in muonic hydrogen. *Phys.Lett.*, 71B, 443.

- Backenstoss, G. 1970. Pionic atoms. *Ann.Rev.Nucl.Sci.*, 467.
- _____, H. Daniel, K. Jentzsch, H. Koch, H.P. Povel, F. Schmeissner, K. Springer, R.L. Stearns. 1971. Muonic x-ray measurements with a high pressure gas target. *Phys. Lett.* 36B, 422.
- _____, T.von Egidy, J. Egger, R. Hagelberg, C.J. Herrlinger, H. Koch, H.P. Povel, Achwitter, L. Tauscher. 1973. Formation of pionic and muonic atoms in liquid helium and hydrogen. In *High-Energy Physics and Nuclear Structure: Proceedings of the Fifth International Conference on High-Energy Physics and Nuclear Structure*, edited by G. Tibell, pp 299-302, North Holland, Amsterdam.
- _____, J. Egger, T. von Egidy, R. Hagelberg, G.J. Herrlander, H.P. Povel, A. Schwitter and L Tauscher. 1974. Pionic and muonic x-ray transitions in liquid helium. *Nucl.Phys.*, 232A, 519.
- _____, A. Brandao d'Oliveira, M. Izycki, H.O. Meyer, I. Schwanner and L. Tauscher; P. Blüm, W. Fetscher, D. Gotta, H. Koch, H. Poth and L.M. Simons. 1977. Pion absorption on ^3He . In abstract volume of the Seventh International Conference on High-Energy Physics and Nuclear Structure, p 283, Sin-Swiss Institute for Nucl. Research, Switzerland.
- Bailey, W.N. 1964. Generalized Hypergeometric Series. Stechert-Hafner Service Agency, Inc. New York.
- _____, A. Placci, E. Polacco, E. Zavatinni, K. Ziock, G. Carboni, U. Gastaldi, G. Carini, G. Neri, G.

- Torelli. 1970. Measurements of pionic x-rays from hydrogen. Phys.Lett., 33B, 369.
- Berezin, S. and G. Bureson, D. Eartly, A. Roberts and T.O. White. 1970. X-rays from μ , π and Σ^- capture in very light elements. Phys.Rev. 2A, 1630.
- Bertin, A. and A. Vitale, A. Placci. 1975. Atomic and molecular processes involving hydrogen and deuterium muonic systems in matter: formation and elastic scattering of μp and μd muonic atoms. Revista del Nuovo Cimento, 5, 423.
- Bethe, H.A. and Salpeter, E.E. 1957. Quantum mechanics of one- and two-electron systems. In Handbuch der Physik, 35, pp 88-436, Springer-Verlag OHG., Berlin.
- _____ and Leon, M. 1962. Negative meson absorption in liquid hydrogen. Phys.Rev., 127, 636.
- Bieniek, J. 1974. Semi-classical uniform approximation in Penning ionization. J.Phys., 7B,
- Blint, R.J. 1976. Spectrum of potential energy curves for the He_2^+ system. Phys. Rev., 14A, 2055.
- Bolden, R.C., R.S. Hemsworth, M.J. Show and N.D. Twiddy. 1970. The measurement of Penning Ionization cross-sections for He 2^3s metastables using a steady-state flowing afterglow method. J.Phys., 3B, 61.
- Buchholz, H. 1969. The Confluent Hypergeometric Function. Springer-Verlag, Berlin.
- Burhop, E.H.S. 1952. The Auger Effect. University Press, Cambridge.

- Burhop, E.H.S. 1969. Mesonic atoms. In High Energy Physics, edited by E.H.S. Burhop, pp 110-281, Academic Press, New York
- Hansen, E.P. . 1970. Exotic atoms. Contemp.Phys., 11, 335.
- Budick, B., J.R. Taraskar, I. Yaghaobia. 1971. Muonic x-rays from liquid hydrogen. Phys.Lett., 34B, 539.
- Burbidge, G.R. and de Borde, A.H. 1953. The Mesonic Auger Effect. Phys.Rev., 89, 189.
- Chattarji, D. 1976. The Theory of Auger Transitions. Academic Press, New York.
- Condo, G.T. 1964. On the absorption of negative pions by liquid helium. Phys.Lett., 9, 65.
- and Borde. 1975. Mass dependence in mesonic atoms. Phys. Rev., 11A, 376.
- Czuchlewski, S.J., Ryan, S.R. and McCucke. 1977. Collisional quenching of metastable hydrogen atoms by atoms and molecules. Phys.Rev., 16A,
- Day, T.B. 1960. K^- meson capture in helium. Nuovo Cimento, 18, 381.
- Eisenberg, Y. and Kessler, D. 1961. On the μ -mesonic atoms. Nuovo Cimento, 19, 1195.
- Fried, Z and Tansey, R.J. 1976. Possible correlations of electromagnetic transitions in exotic atoms and their implications for cascade calculations. Phys.Lett., 63B, 245.
- Garrison, B.J., W.H. Miller and H.F. Schaefer. 1973. Penning and associative ionization of triplet metastable

- helium atoms. *J.Chem.Phys.*, 59, solutions. *Phys.Rev.*,
- Haff, P.K. and Tombrello, T.A. 1974. Negative muon capture
in very light atoms. *Ann. of Phys.*, 86, 178. University
- Hansen, E.R. 1975. A Table of Series and Products. Prentice-
Hall, Inc., New Jersey. M. Leon, J. Miller, 1976. Atomic
- Hickman, A.P. and Mergner, H. 1977. Calculation of associ-
ative and Penning ionization of H and D by He(2^1S) and
He(2^3S). *J.Chem.Phys.*, 67, 5484 ic hydrogen. *Phys.Lett.*,
- Hughes, V.W., R.O. Mueller, H. Rosenthal and C.S. Wu. 1975.
Collision quenching of the metastable 2S state on muonic
hydrogen and the muonic helium ion. *Phys. Rev.*, 11A,1175.
- Huo, Winifred M. 1977. On the equivalence of semiclassical
and Born total cross sections. Penning ionization of
H(1^2S) by He(2^1S). *J.Chem.Phys.*, 67, 5624 Observed
- Kalinin, A.P. and Leonas, V.B. 1977. Study of ionization in
slow collisions of atomic particles. *Sov.Phys.Usp.*, 20,279
- Kaplan, S.N., L.F. Mausner, J.A. Monard and R.A. Naumann.
1975. Chemical effects in the capture of negative muons.
Phys.Lett., 56B, 145. ionic helium three. In abstract
- Kim, Y.N. 1971. Mesic Atoms and Nuclear Structure. North-
Holland, Amsterdam. Nuclear Structure, p 236, Sin-Swiss
- Knight, J.D. and L.F. Mausner, R.H. Naumann, C.J. Orth and
M.E. Schillaci. 1977. Hydrogen isotope effect on muonic
x-ray spectra of $(CH_2)_X$ and H_2O . *Phys.Rev.Lett.*, 38, 953.
- _____, C.J. Orth, M.E. Schillaci, R.A. Naumann, H.
Daniel, H.B. Knowles and K. Springer. 1976. Chemical
effects in negative muon capture in some ionic and co-

valent solids and ionic aqueous solutions. Phys.Rev.,
13A, 43.

Kunselman, A.R. 1969. Pionic Atoms. Ph.D. Thesis. University
of California, Berkeley.

_____ and J. Low, M. Leon, J. Miller. 1976. Atomic
structure effects in negative meson capture. Phys.Rev.
Lett., 36, 446.

Leon, M. 1971. X-ray yields in muonic hydrogen. Phys.Lett.,
35B, 413.

_____ and Seki, R. 1977. Atomic capture of negative
mesons I, II. Nucl.Phys., 282A, 445.

Luke, Y.L. 1969. The Special Functions and Their Approx-
imations, volumes I and II. Academic Press, New York.

Lum, G.K., C.E. Wiegand and G.L. Godfrey. 1976. Observed
isotropy in pionic argon x-ray angular distribution. Phys.
Lett., 65B, 43.

Mason, G.R., S.K. Kim, G.A. Beer, A. Olin, R.M. Pearce; D.A.
Bryman, M.S. Dixit, J.A. Macdonald and J.S. Vincent.

1977. X rays from pionic helium three. In abstract
volume of the Seventh International Conference on High-
Energy Physics and Nuclear Structure, p 286, Sin-Swiss
Institute for Nuclear Research, Switzerland.

Michael, D.N. 1967. K-mesonic x-rays and K^- absorption in
liquid helium. Phys.Rev., 158, 1343.

Miller, W.H. 1970. Theory of Penning ionization: I.Atoms.
J.Chem.Phys., 52, 3563

_____ and Schaefer, H.F. 1970. Theoretical treat-

ment of Penning ionization. He (1s 2s ¹S, ³S) + effect
H(1s ²S)*. J.Chem.Phys., 53,

_____ and C.A. Slocomb, H.F. Schaefer. 1972. G. Carboni,

Molecular autoionization lifetimes and cross-sections
for Penning ionization: numerical results for
He*(1s 2s ³S) and H(1s ²S)*. J.Chem.Phys., 56, 1347

_____ and Morgner. 1977. A unified treatment of
Penning ionization and excitation transfer. J.Chem.Phys.,
67,

McCusker, M.V. 1977. Collisional quenching of metastable
hydrogen atoms by atoms and molecules. Phys.Rev., 16A,

Niehaus, A. 1973. Penning ionization. Berichte der Bunsen-
Gesellschaft, 77, 632

Mausner, L.F. 1975. Chemical effects on the atomic capture
of negative muons. Ph.D. Thesis. Princeton University,
Princeton.

Messiah, A. 1958. Quantum Mechanics, I and II. Wiley, New
York.

Pfeiffer, H.J., K. Springer, H. Daniel. 1975. Intensitäten
Myonischer Röntgenlinien in Argon, in Wasserstoff Plus
Argon und in Argon Plus Neon. Nucl.Phys., 254A, 433.

_____, K. Springer, G. Backenstoss, H. Daniel. 1975.
Pionic x-rays from argon and hydrogen plus argon.
Z.Phys., 275A, 369.

Placci, H., E. Polacco, E. Zauattini, K. Ziuck, C. Carboni,
U. Gastaldi, G. Gorini and G. Torelli. 1970. Observation
of muonic x-rays in hydrogen gas. Phys.Lett., 32B, 413.

- _____ et al. 1973. Measurement of the Auger effect in $(\mu^4\text{He})_{2s}^+$ ionic system. Lett. Nuovo Cimento, 6, 233.
- _____, E. Polocco, E. Zavattini, K. Ziuck, G. Carboni, U. Gastaldi, G. Gorini, G. Neri, G. Torelli. 1971. Observation of muonic x-rays in helium gas and measurement of the two photon decay rate of the 2s metastable state. Nuovo Cimento, 1A, 445.
- Ponomarev, L.I. 1973. Molecular structure effects on atoms and nuclear capture of mesons. Ann.Rev.Nucl.Sci., 395.
- Rudermann, M.A. 1960. X-ray yields from μ -mesic atoms. Phys. Rev., 6, 1630.
- Russell, J.E. 1965. Capture of negative mesons in liquid helium. Proc.Phys.Soc., 85, 245.
- _____ (A) 1970. Structure of neutral mesonic atoms formed in liquid helium. Phys.Rev., 1A, 721.
- _____ (B) 1970. Distortion of the electron wave function in $\alpha\pi^-e^-$, αK^-e^- , αp^-e^- atoms. Phys.Rev., 1A, 735.
- _____ (C) 1970. Auger rates for circular orbits of $\alpha\pi^-e^-$, αK^-e^- , αp^-e^- atoms. Phys.Rev., 1A, 742.
- _____. 1975. Fried-Martin corrections for Mesonic Auger transitions. Phys. Lett., 55B, 459.
- Sack, R.A. 1961. Two-center expansion for the powers of the distance between two points. J.Math.Phys., 5, 260.
- Sapp, B.O. 1974. Observation of K-series transitions in pionic and muonic ^3He atoms. WM 74-50. The College of William and Mary in Virginia.

- Schucan, T.H. 1977. Interference between multi-step transitions in exotic atoms. Phys.Lett., 69B, 293.
- Seki, R. and Wiegand, C. 1975. Kaonic and other exotic atoms. In Annual Review of Nuclear Science, edited by E. Segre, 25, pp 241-282, Annual Reviews, Inc., Palo Alto, Calif.
- Slater, L.J. 1960. Confluent Hypergeometric Functions. The University Press, Cambridge.
- Sluckin. T.J. 1977. Positive ion structure in ^3He -rich liquid helium mixtures. Phys.Lett., 64A, 211.
- Tansey, R.J. 1975. Coherent radiative transitions in mesic atoms. Lowell Technological Institute Ph.D. Thesis, University Microfilms, 75-26,385, Ann Arbor.

APPENDIX A

HYPERGEOMETRIC FUNCTIONS

The following is a brief and by no means complete introduction to hypergeometric functions.

A.1 Definition of Hypergeometric Functions

The gamma function can be defined by Euler's integral

$$\Gamma(z) = \int_0^{\infty} e^{-t} t^{z-1} dt \quad \text{Re}(z) > 0 \quad (\text{A.1})$$

Partial integration of (A.1) shows that $\Gamma(z)$ satisfies the difference equation

$$\Gamma(z+1) = z \Gamma(z) \quad (\text{A.2})$$

and since $\Gamma(1) = \Gamma(2) = 1$

$$\Gamma(n+1) = 1 \cdot 2 \cdot \dots \cdot n = n! \quad (\text{A.3})$$

It is convenient at this point to introduce

Pochhammer's Symbol $(a)_k$

$$(a)_k = a(a+1)\dots(a+k-1) \quad (a)_0 = 1 \quad (\text{A.4})$$

$$(a)_j = \frac{\Gamma(a+j)}{\Gamma(a)} \quad a \neq \text{negative integer}$$

$$= (-1)^j \frac{\Gamma(1-a)}{\Gamma(1-a-j)} \quad a \neq \text{positive integer}$$

Then the formulae

$$(a)_{n+k} = (a+n)_k (a)_n \quad (\text{A.5})$$

$$(a)_{n-k} = \frac{(-1)^k (a)_n}{(1-a-n)_k} \quad (\text{A.6})$$

are easily proved for integer values of n and k . Noting that $(-n)_k$ is zero whenever $k > n$, the binomial coefficient can be defined as

$$\binom{n}{k} = \frac{(-1)^k (-n)_k}{k!} \quad (\text{A.7})$$

Other properties of the gamma function which will be useful are

$$\Gamma(z) \Gamma(1-z) = \frac{\pi}{\sin \pi z}$$

$$\Gamma(1/2) = \pi^{1/2} \quad (\text{A.8})$$

$$\Gamma(2z) = 2^{2z-1} \Gamma(z) \Gamma(z+1/2) / \Gamma(1/2)$$

Using (A.8) with $z = 1 + i\gamma$, it can be shown that

$$|\Gamma(1+i\gamma)|^2 = \frac{\pi \gamma}{\sinh \pi \gamma} (1+\gamma^2)(4+\gamma^2)\dots(l^2+\gamma^2) \quad (\text{A.9})$$

A hypergeometric function of one variable is defined by

$${}_pF_q(a_1, a_2, \dots, a_p; c_1, c_2, \dots, c_q; z) = \sum_{j=0}^{\infty} \frac{(a_1)_j (a_2)_j \dots (a_p)_j}{(c_1)_j (c_2)_j \dots (c_q)_j} \frac{z^j}{j!} \quad (\text{A.10})$$

The a 's and c 's are called numerator and denominator parameters, respectively, and z is called the variable.

The ${}_pF_q$ series terminates and, therefore, is a polynomial if a numerator parameter is a negative integer or zero.

i.e.

$${}_2F_1(-m, b; c; z) = \sum_{n=0}^m \frac{(-m)_n (b)_n}{(c)_n n!} z^n \quad (\text{A.11})$$

If $c = -k$, then the hypergeometric function is still defined provided $k \geq m$

$${}_2F_1(-m, b; -m-l; z) = \sum_{n=0}^m \frac{(-m)_n (b)_n}{(-m-l)_n n!} z^n \quad (\text{A.12})$$

If none of the numerator or denominator parameters is a negative integer or zero, then application of the ratio test shows that the series

converges for all finite z if $p \leq q$

converges for $|z| < 1$ if $p = q + 1$ (A.13)

diverges for all z , $z \neq 0$, if $p > q + 1$

Furthermore if

$$\eta = \sum_{n=1}^p a_n - \sum_{n=1}^q c_n \quad (\text{A.14})$$

then the series ${}_qF_{q-1}$ is

absolutely convergent for $|z| = 1$ if $R(\eta) > 0$

conditionally convergent for $|z| = 1$, $z \neq 1$ if $0 \leq R(\eta) \leq 1$

divergent for $|z| = 1$ if $1 \leq R(\eta)$ (A.15)

The hypergeometric function most commonly encountered are the confluent hypergeometric function ${}_1F_1(a; c; z)$ and

the Gauss hypergeometric function ${}_2F_1(a, b; c; z)$ and are, in fact, the two of concern in the present study.

A.2 Examples of Hypergeometric Functions

Many elementary and special functions are expressible as hypergeometric functions. For example, there are the elementary functions

$$z^a = {}_2F_1(-a, b; b; 1-z)$$

$$e^z = {}_1F_1(a; a; z)$$

$$\sin z = z e^{-iz} {}_1F_1(1; 2; -2iz)$$

$$\ln(1-z) = -z {}_2F_1(1, 1; 2; z)$$

the Laguerre and Legendre Polynomials

$$L_n^{(\alpha)}(x) = \frac{(\alpha+1)_n}{n!} {}_1F_1(-n; \alpha+1; x)$$

$$P_l^m(\cos \theta) = \left(-\frac{\sin \theta}{2}\right)^m \frac{(m+l)!}{(l-m)! m!} {}_2F_1(-l+m, m+l+1; m+1; \frac{1-\cos \theta}{2})$$

and the spherical Bessel functions and the Coulomb Wave Functions

$$j_l(z) = \frac{\Gamma(l+1)}{\Gamma(2l+2)} (2z)^l e^{-iz} {}_1F_1(l+1; 2l+2; 2iz)$$

$$F_l(\eta, \rho) = Q_l(\eta) \rho^{l+1} e^{-i\rho} {}_1F_1(l+1-i\eta; 2l+2; 2i\rho)$$

$$\Psi_c = e^{-\frac{1}{2}\pi\eta} \Gamma(1+i\eta) e^{i\vec{k}\cdot\vec{r}} {}_1F_1(-i\eta; 1; ikr - i\vec{k}\cdot\vec{r})$$

A.3 Derivatives and Differential Equations

For the Confluent hypergeometric function, the derivative is simply

$$\frac{d^n}{dz^n} \left\{ {}_1F_1(a; b; z) \right\} = \frac{(a)_n}{(b)_n} {}_1F_1(a+n; b+n; z) \quad (\text{A.16})$$

and the differential equation is

$$z \frac{d^2 \omega}{dz^2} + (b-z) \frac{d\omega}{dz} - a\omega = 0 \quad (\text{A.17})$$

For the Gauss hypergeometric function, they are given by

$$\frac{d^n}{dz^n} \left\{ {}_2F_1(a, b; c, z) \right\} = \frac{(a)_n (b)_n}{(c)_n} {}_2F_1(a+n, b+n; c+n; z) \quad (\text{A.18})$$

$$z(1-z) \frac{d^2 \omega}{dz^2} + [c - (a+b+1)z] \frac{d\omega}{dz} - ab\omega = 0 \quad (\text{A.19})$$

A.4 Recurrence relations for the Gauss Hypergeometric Function.

The six functions ${}_2F_1(a+1, b; c; z)$, ${}_2F_1(a, b+1; c; z)$, ${}_2F_1(a, b; c+1; z)$ are called contiguous to ${}_2F_1(a, b; c; z)$. Relations between ${}_2F_1(a, b; c; z)$ and any two contiguous functions have been given by Gauss. By repeated application of these relations the function ${}_2F_1(a+m, b+n; c+1; z)$ with integer $m, n, 1$ can be expressed as a linear combination

of ${}_2F_1(a, b; c; z)$ and one of its contiguous functions with coefficients which are rational functions of a, b, c, z .

A.5 Linear Transformations

The simplest and perhaps most useful transformation of the Gauss hypergeometric function is

$${}_2F_1(a, b; c; z) = (1-z)^{-a} {}_2F_1(a, c-b; c; \frac{z}{z-1}) \quad (\text{A.20})$$

others are

$$\begin{aligned} {}_2F_1(a, b; c; z) &= \frac{\Gamma(c) \Gamma(c-a-b)}{\Gamma(c-a) \Gamma(c-b)} {}_2F_1(a, b; a+b-c+1; 1-z) \\ &+ (1-z)^{c-a-b} \frac{\Gamma(c) \Gamma(a+b-c)}{\Gamma(a) \Gamma(b)} {}_2F_1(c-a, c-b; c-a-b+1; \frac{1-z}{z}) \end{aligned} \quad (\text{A.21})$$

$$\begin{aligned} &= \frac{\Gamma(c) \Gamma(b-a)}{\Gamma(b) \Gamma(c-a)} (-z)^{-a} {}_2F_1(a, 1-c+a; 1-b+a; \frac{1}{z}) \\ &+ \frac{\Gamma(c) \Gamma(a-b)}{\Gamma(a) \Gamma(c-b)} (-z)^{-b} {}_2F_1(b, 1-c+b; 1-a+b; \frac{1}{z}) \end{aligned} \quad (\text{A.22})$$

$$\begin{aligned} &= (1-z)^{-a} \frac{\Gamma(c) \Gamma(b-a)}{\Gamma(b) \Gamma(c-a)} {}_2F_1(a, c-b; a-b+1; \frac{1}{1-z}) \\ &+ (1-z)^{-b} \frac{\Gamma(c) \Gamma(a-b)}{\Gamma(a) \Gamma(c-b)} {}_2F_1(b, c-a; b-a+1; \frac{1}{1-z}) \end{aligned} \quad (\text{A.23})$$

$$\begin{aligned} &= \frac{\Gamma(c) \Gamma(c-a-b)}{\Gamma(c-a) \Gamma(c-b)} z^{-a} {}_2F_1(a, a-c+1; a+b-c+1; 1-\frac{1}{z}) \\ &+ \frac{\Gamma(c) \Gamma(a+b-c)}{\Gamma(a) \Gamma(b)} (1-z)^{c-a-b} z^{a-c} {}_2F_1(c-a, 1-a; c-a-b+1; 1-\frac{1}{z}) \end{aligned} \quad (\text{A.24})$$

These transformations may also be used (with extreme care) when $a = -m$, i.e.

$${}_2F_1(-m, b; c; z) \quad (\text{A.25})$$

$$= \frac{(b)_m}{(c)_m} (-z)^m {}_2F_1(-m, 1-m-c; 1-m-b; \frac{1}{z})$$

A.6 Summation Formula

For $z = 1$, the Gauss summation theorem states

$${}_2F_1(a, b; c; 1) = \frac{\Gamma(c) \Gamma(c-a-b)}{\Gamma(c-a) \Gamma(c-b)} \quad (\text{A.26})$$

c not a negative integer or zero; $R(c-a-b) > 0$

If a or b is a negative integer, we have the result known as Vandermonde's theorem

$${}_2F_1(-n, b; c; 1) = \frac{(c-b)_n}{(c)_n} \quad (\text{A.27})$$

c not a negative integer or zero

If c is a negative integer or zero, say $c = -m$, and $m > n$, then

$$\sum_{k=0}^n \frac{(-n)_k (b)_k}{(-m)_k k!} = \frac{(m-n)! (m+b+1-n)_n}{m!} \quad (\text{A.28})$$

While theorems like this last may seem distant to the uninitiated, when written in the more familiar notation of binomial coefficients, they become more comprehensible.

For example (A.28) becomes

$$\binom{b+1+m}{n} = \sum_{k=0}^n \binom{b+k}{b} \binom{m-k}{m-n} \quad (\text{A.29})$$

While many sum formulae exist, only two will be given here since only these are used in the text.

$$\sum_{z=0}^{\infty} \frac{(d)_z}{z!} y^z {}_2F_1(-z, b; c; x)$$

$$= (1-y)^{-d} {}_2F_1(d, b; c; \frac{xy}{y-1}) \quad (\text{A.30})$$

$$\sum_{k=0}^{\infty} \frac{(a)_k (b)_k}{(c)_k k!} y^k {}_2F_1(1-a, c-a; 1-a-k; x)$$

$$= (1-x)^{a+b-c} (1-x+xy)^{-b} {}_2F_1(a, b; c; \frac{y}{1-x+xy}) \quad (\text{A.31})$$

These and most other sum formulae for hypergeometric functions can be derived by using three basic techniques;

- 1) rearrangement of terms
- 2) expansion in Taylor series, and
- 3) Vandermonde's theorem.

A.7 Integration of Confluent Hypergeometric Functions

Of immediate concern is the integral

$$\int_0^{\infty} x^{b-1} e^{-sx} {}_1F_1(a; c; kx) dx = \frac{\Gamma(b)}{s^b} {}_2F_1(a, b; c; k/s)$$

$$[|s| \geq |k| \quad \text{Re } b > 0] \quad (\text{A.32})$$

When the convergence conditions are not met (i.e. $|s| < |k|$) then an answer can be obtained by using the ${}_2F_1$ function for those values when it converges, transforming it to a function which does converge for all values of the parameters, then using analytic continuation to extend the solution for all values of the parameters.

For example

$$\int_0^{\infty} x^{b-1} e^{-(i+\gamma)x} {}_2F_1(a+i\gamma; c; 2ix) dx$$

$$= \frac{\Gamma(b)}{(i+\gamma)^b} {}_2F_1(a+i\gamma, b; c; \frac{2i}{i+\gamma}) \quad (\text{A.33})$$

which converges only for $|i+\gamma| > |2i|$, $\gamma > \sqrt{3}$.

Now there is no possible physical explanation why the integral, which is related to the transition rate calculation, should diverge when the energy of the final electron is less than 1.5 ev. Therefore, since b and c are integers, and $b > c$, then

$$\frac{\Gamma(b)}{(i+\gamma)^b} {}_2F_1(a+i\gamma, b; c; \frac{2i}{i+\gamma})$$

$$= \frac{\Gamma(b)}{(i+\gamma)^b} \left(1 - \frac{2i}{i+\gamma}\right)^{-(a+i\gamma)} {}_2F_1(a+i\gamma, c-b; c; \frac{2i}{i-\gamma})$$

$$= \frac{\Gamma(b)}{(i+\gamma)^b} \left(\frac{\gamma-i}{\gamma+i}\right)^{-a-i\gamma} \sum_{n=0}^{b-c} \frac{(a+i\gamma)_n}{(c)_n} \frac{(c-b)_n}{n!} \left(\frac{2i}{i-\gamma}\right)^n$$

which converges for all values of γ .

(A.34)

APPENDIX B

ENERGIES AND SCREENING FACTORS FOR SOME CIRCULAR ORBITS
OF PIONIC HELIUM¹

N_{π}	E (R)	E (M)	Z_e (R)	Z_e (M)	Z_{π} (R)	Z_{π} (M)
12	-8.4	-8.42	1.14	1.16	1.97	1.97
14	-6.573	-6.559	1.26	1.23	1.92	1.94
15	-5.954	-5.940	1.38	1.42	1.86	1.83
16	-5.487	-5.477	1.52	1.49	1.75	1.78
17	-5.149	-5.130	1.71	1.71	1.55	1.56

Energies are in Rydbergs (1 Rydberg = 13.6 ev.)

¹ This table is taken from Mausner (1975) p.57.

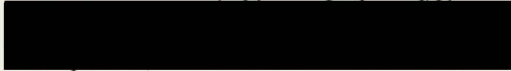
PARTIAL COPYRIGHT LICENSE

I hereby grant the right to lend my thesis (the title of which is shown below) to users of the University of Victoria Library, and to make single copies only for such users or in response to a request from the library of any other university, or similar institution, on its behalf or for one of its users. I further agree that permission for extensive copying of this thesis for scholarly purposes may be granted by me or a member of the University designated by me. It is understood that copying or publication of this thesis for financial gain shall not be allowed without my written permission

Title of Thesis

THEORY OF THE MESIC AUGER EFFECT

Author


Elizabeth Ann Miller

April 27, 1979